

Use Authorization

In presenting this thesis in partial fulfillment of the requirements for an advanced degree at Idaho State University, I agree that the Library shall make it freely available for inspection. I further state that permission to download and/or print my thesis for scholarly purposes may be granted by the Dean of the Graduate School, Dean of my academic division, or by the University Librarian. It is understood that any copying or publication of this thesis for financial gain shall not be allowed without my written permission.

Signature _____

Date _____

DEVELOPING A CONSTANT DISCHARGE STRUCTURE FOR
DETENTION BASIN OUTLET THAT WILL ALLOW DETENTION
BASIN VOLUME TO BE MINIMIZED

by

Ahmed Alhaddad

Purposely Submitted in Partial Fulfillment

of the Requirements for the Degree

Master of Science in the Department of Civil and Environmental Engineering

Idaho State University

Summer 2014

To the Graduate Faculty:

The members of the committee appointed to examine the thesis of Ahmed Kamel Alhaddad find it satisfactory and recommend that it be accepted.

Dr. Bruce Savage,
Major Advisor

Dr. Arya Ebraminpour,
Committee Member

Dr. Brian Williams,
Graduate Faculty Representative

Acknowledgements

For the past two years, I have dedicated my time to Idaho State University, and have had a great journey filled with learning and experience. I would like to give special thanks to my committee members, starting with my advisor Dr. Bruce Savage, who has never stopped inspiring me. I would like to thank him for encouraging my research and guiding me toward success. I have learned from him what books and written literature have failed to teach. He has provided me with endless knowledge without asking for anything in return. I would also like to thank Dr. Arya Ebrahimpour for offering his help all the time and assisting me when I needed guidance. He was the first ISU faculty member I met, and at that time I knew that I made the right decision applying to this school. I also want to thank Dr. Brian Williams in advance for reading and critiquing my work. The pleasure is mine, having him evaluating my work.

This research would not have been possible without the use of different Idaho State University facilities. I would like to thank the College of Science and Engineering for the \$2,000 grant that funded the materials used in my physical model. Also, I have to mention and thank them for the access they gave me to the computer lab in the engineering building, where I worked on the SolidWorks 3D model. Special thanks from me to the Civil Engineering department, which has provided me with access to a students' office equipped with a state-of-the-art computer, where I spent most my time researching and working on the Flow-3D simulation model. I would like to thank them for giving me access to the Flume Laboratory where I assembled my physical model. I was lucky to have Dr. Bruce as my advisor, as he spent some of his time assuring himself that my time spent at the university was as comfortable as possible. I would also like to thank the Saudi

Arabian Cultural Mission (SACM) for my scholarship, which covered most of my financial needs.

Finally, I would like to thank those without whom my accomplishments would have not been possible, for their moral support and encouragement: my parents, family members, friends and instructors. They have always been there to support me, to the point that I sometimes forget that someone is always there to help me. To me, they are the infrastructure of my life; life without them would be meaningless and worthless. I hope my research and work has met their expectations of me.

Table of contents:

	Page
List of Figures	viii
Abstract	xi
Chapter 1 – Introduction to Detention Basin Outlet	1
1.1 Purpose	1
1.2 Background	1
1.2.1 Basic Hydrology	1
1.2.2 Land Development	4
1.2.3 Reducing the flood potentials caused by land developments	6
1.2.4 Detention Basins	8
1.2.5 Types of Detention Basins and estimating the volume of the storage area	10
Chapter 2 – Literature Review for the controlled flow detention basins	13
2.1 Outlet Controlling Water flow Regulators	13
2.1.1 Orifice Plate	13
2.1.2 Steinscrew	14
2.1.3 Hydro-Brake System (Vortex Valves)	16
2.1.4 Wirbeldrossel	17
2.1.5 The Flow valve	19
2.1.6 Mechanical Floating Outlets	20
2.1.7 Detention Basin Outlet Structure (DBOS)	23
2.2 General controlled outlet design aspects and consecrations	25
2.2.1 Hydraulic Function	25
2.2.2 Water Quality Considerations	26
2.2.3 Safety	26
2.2.4 Maintenance	26
2.2.5 Aesthetics	27
Chapter 3 – Computational Fluid Dynamics	28
3.1 Governing Equation	28
3.2 Numerical Approximations	30
3.3 Meshing	32
Chapter 4 – Methods	34
4.1 Mechanical Floating Outlet device	34
4.1.1 Flow-3D models	36
4.1.1.1 General Moving Objects overlapping at time step zero	36

4.1.1.2 General Moving Objects with No Overlapping at Time Step Zero	42
4.1.2.3 Hose Buckling	45
Chapter 5 – Results and Calculations	58
5.1 Physical Models	58
5.2 Weirs Discharge Coefficient	62
5.3 Comparing the Physical Model Data to RSC Equation Results	66
Chapter 6 – Conclusions and Recommendations	69
References	71
Appendix	74

List of Figures:

	Page
Figure 1-1 Dimensionless hydrograph	3
Figure 1-2 Post and pre-development hydrographs (McCuen, 2005)	5
Figure 1-3 Diagram of a detention basin (Olsen, 2004)	8
Figure 1-4 Improved developed drainage basin using detention basin (Ferguson, 1998)	9
Figure 1-5 Most effective use of the detention basin storage area hydrograph (red). After vs before development hydrograph (Black). (McCuen, 2005) modified	9
Figure 1-6 Subscript 1 and 2 in the energy equation (Olsen, 2004) modified	11
Figure 2-1 Orifice Plate configuration (Dermot, 2008)	13
Figure 2-2 Steinscrew flow regulator (Urbonas and Stahre 1993)	14
Figure 2-3 Performance of four regulators in series (Urbonas and Stahre 1993)	15
Figure 2-4 Vortex initiation phase (A). Head Versus Flow Characteristics For vortex valve controlled discharge (B) (Hydro International, 2012).	16
Figure 2-5 Wirbeldrossel (left) and Wirbelvalve (right) flow regulators (Urbonas and Stahre, 1993).	18
Figure 2-6 flow capacity of Wirbeldrossel vs. an orifice (Urbonas and Stahre, 1993).	18
Figure 2-7 The Flow valve installed inside a manhole (Left). The discharge curve of the flow valve versus an orifice flow (Right) (Urbonas and Stahre, 1993).	19
Figure 2-8 An example of floating outlet flow regulator (Urbonas and Stahre, 1993).	20
Figure 2-9 Patented self-regulating fluid flow valves (HARDY, 1968).	21
Figure 2-10 HydrOslide flow regulator (HYDROK, 2014)	22
Figure 2-11 Layout of the Detention Basin Outlet Structure (Olsen, 2004)	23

Figure 2-12 Theory vs. real model discharge flow results for the outlet structure with external (differential) pressure on the flexible gate (Olsen, 2004).	24
Figure 4-1 Schematic drawing of the regulator location.	35
Figure 4-2 Transparent FAVOR view of the solid object inside the controlled volume (blue lines).	37
Figure 4-2 Different time step for General moving objects overlapping at time step zero After water reached a certain elevation (at 56 sec) the water depth above the slate opening stayed constant.	40
Figure 4-3 Operating flow over variable head using General Moving Objects overlapping at time step zero simulation	41
Figure 4-4 The initial time frames of no overlapping GMO simulation shows the moving pipe kept rising through the rigid floor.	43
Figure 4-5 advance time frames of no overlapping GMO simulation shows the physically impossible behavior of the moving pipe.	44
Figure 4-6 Series of stabilized flow simulations at different fixed pipe heads	46
Figure 4-7 Vertical cross section of the telescopic pipes layout	47
Figure 4-8 3D SolidWorks, 360 Photoview. The proposed flow regulator	48
Figure 4-9 Original physical model set-up	50
Figure 4-10 The constructed circular track	51
Figure 4-11 Water outside the hose is used to counter the water pressure inside the hose	53
Figure 4-12 Hose is buckling with the water counter pressure approach used.	54
Figure 4-13 light weigh slot attached to the floater and the hose is sported by four vertical pipes.	56
Figure 4-14 Hose is buckling and leaning toward the supporting pipes	57
Figure 5-1 The flow regulator, three trails flow output at different pressure head.	59
Figure 5-2 The average weight change at different heights	61
Figure 5-3 Streamlines showing the flow direction for the horizontal flow	63
Figure 5-4 Streamlines showing the flow direction for the vertical flow	64

Figure 5-5 Flow rate at different water heads when increasing the pressure head using different methods. 65

Figure 5-6 Comparing the physical model flow data to the rectangular sharp crest weir equation with weight factored in. 67

Abstract

Developing a Mechanical Constant Flow Regulator Structure for Detention Basin Outlet
Thesis Abstract – Idaho State University (2014)

In a storm event on developed land, a detention basin will store a variable volume of water while releasing some water. The discharged flow rate must be less than the peak flow prior to the land development to prevent flooding. However, stored water will gain potential energy as it rises inside the detention basin forcing more water flow out of the storage basin. This phenomenon causes engineers to restrict the outlet culvert to a smaller diameter and requires a larger area for storage. Engineers have developed detention flow regulators to reduce the area needed for the storage basin.

This research project proposes and analyzes a new outlet regulator used for developing a constant outflow for a detention basin. The mechanical outflow regulator consists of a floating duct hose that moves vertically to maintain constant hydraulic head difference. A computer simulation, using FLOW-3D software, was developed prior to the physical model to insure workability and to optimize the model.

The overall results show a regulated flow when the total head is increased. Therefore, the volume of the detention basin can be reduced without lowering overflow values. The proposed flow regulator is a promising concept to control the outflow of a detention basin that will lead to more refinements and research. The simplicity of the design gives it a cost advantage over other available flow regulators.

Chapter 1 – Introduction to Detention Basin Outlet

1.1 Purpose

As land developed more impervious surfaces constructed increasing the peak discharge rate and the speed of runoff, creating a higher flood potential for cities and towns. To store the difference between the post development peak discharge and the predevelopment peak discharge, engineers have designed water storage areas, called detention basins. A detention basin's outlet is designed to release a flow rate equal to the pre-development peak discharge, when the storage basin is near full for a given design flood. The outlet flow rate is often a function of the stored water depth. The potential energy of the stored water decreases when the water drains out of the basin causing the outlet flow to decrease. This means that a less variable flow can be achieved by using a wide detention basin, but at expense of potential energy, since water depth is reduced. The shortage and the cost of land have motivated engineers to design flow regulators that maintain a constant flow rate as the water storage drains. The focus of this research is to develop a device to release water at a constant discharge rate when the hydraulic head in the storage is changing. This device will reduce the volume needed to store the storm water thereby requiring less land.

1.2 Background

1.2.1 Basic Hydrology

From the time when humans started to settle and urbanize, quantifying and estimating water runoff has been important for managing fresh water resources in order to avoid possible flood hazards (Hubbart, 2008). Hydrologists have used the hydrologic

cycle to measure the magnitude of water runoff. Water evaporates from water surfaces such as oceans and lakes to form clouds. Winds transport clouds, to reach a higher ground elevation. Then, water vapor starts to condense, forming rain, snow and hail. The ground topography and gravity move rainwater and melted snow or ice to lower land, where it congregates to form streams and rivers. The ground topography combined with the soil permeability and vegetation, will determine the rate of water infiltration that forms ground water. Gravity (g) forces water to flow to lower elevations, moving it back to oceans and lakes. Typically, the ground on which water precipitates consists of many dips and rises, forcing water to flow in many small streams in a pattern that looks like blood vessels or like leaf veins called a watershed or drainage basin. Each drainage basin is adjacent to another basin, and they can be distinguished from each other by the distinctive last target stream. In other words, if a raindrop landed in one drainage basin, it would end up in a stream not related to any adjacent drainage basins (Gribbin, 2007).

A hydrograph is a graph used by engineers and hydrologists to determine the relationship between the magnitude of rainfall or run-off and the duration of a storm event at a given point on a stream or river (see Figure 1-1).

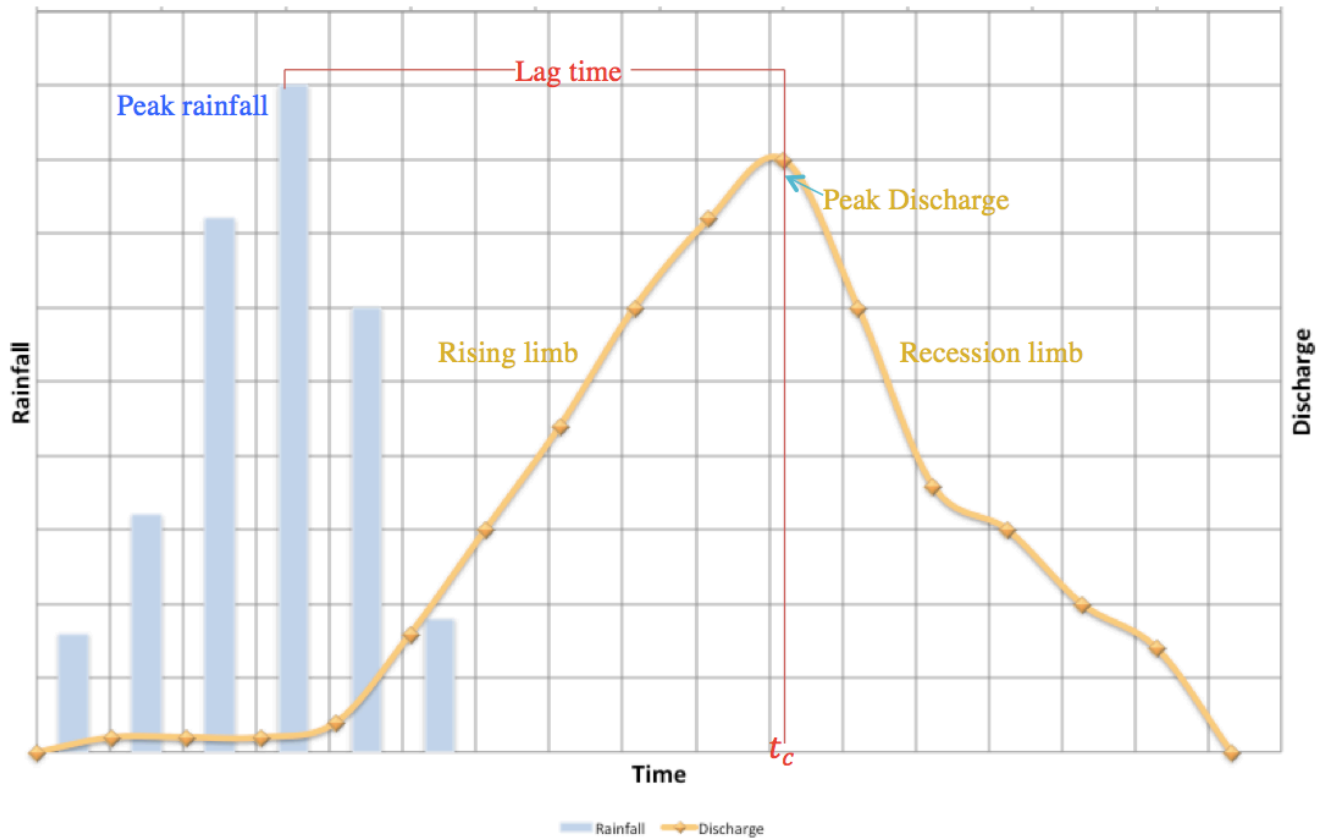


Figure 1-1 General dimensionless hydrograph.

Where:

t_c is the time of concentration.

To explain the shape of the hydrograph's curve, suppose rain falls on ground that has dry soil. At the beginning of the storm, there will be some rainwater losses counted for in the hydrograph, due to the process of making the soil wet. Now, consider a constant rainfall. The magnitude of runoff flow rate will keep increasing, until the farthest raindrop reaches the point of analysis. The flow rate reaches the highest magnitude when run-off at all areas of drainage contributes to the outflow. Time of

concentration (t_c) is the time required for a water drop to flow from the farthest point of the watershed to the outlet, after all the elements of the watershed have contributed to the flow, minus the initial abstraction and infiltration. Time to Peak (T_p) is the duration from the point when the rain event started, to when the flow reaches its peak flow. The rate of infiltration is a function of soil type and vegetation and the water head above the ground as explained by Darcy's Law (Hendriks, 2010):

$$f = K \left[\frac{h_0 - (-\psi - L)}{L} \right] \quad \text{Equation 1}$$

where,

f is the rate of infiltration

ψ is wetting front soil suction head

h_0 is the depth of ponded water above the ground surface

K is the hydraulic conductivity

L is the total depth of subsurface ground in question

1.2.2 Land Development

Land development is responsible for an increase in the peak discharge rate, which causes a higher potential for flooding to occur downstream from the drainage basin (See Figure 1-2). For instance, the removal of trees and vegetation decreases the amount of water stored on their surface, which is called initial abstraction. Similarly, site grading and soil compaction will reduce the infiltration rate and the water stored in the soil matrix. Moreover, non-pervious surfaces (such as asphalt, concrete, brick, and stone) used for land development increase the run-off rate by reducing the water storage and infiltration rate. The non-porous surfaces will reduce the Time of concentration (T_c) and

decrease the time it takes for run-off to reach the water shed outlet and cause a higher peak discharge rate. In conclusion, land development impact can be summarized as

(McCuen, 2005):

- 1- Faster and higher peak flows.
- 2- More flow volume at higher average velocity during storm event and lower base flow.
- 3- Greater level of pollution and higher average temperature.

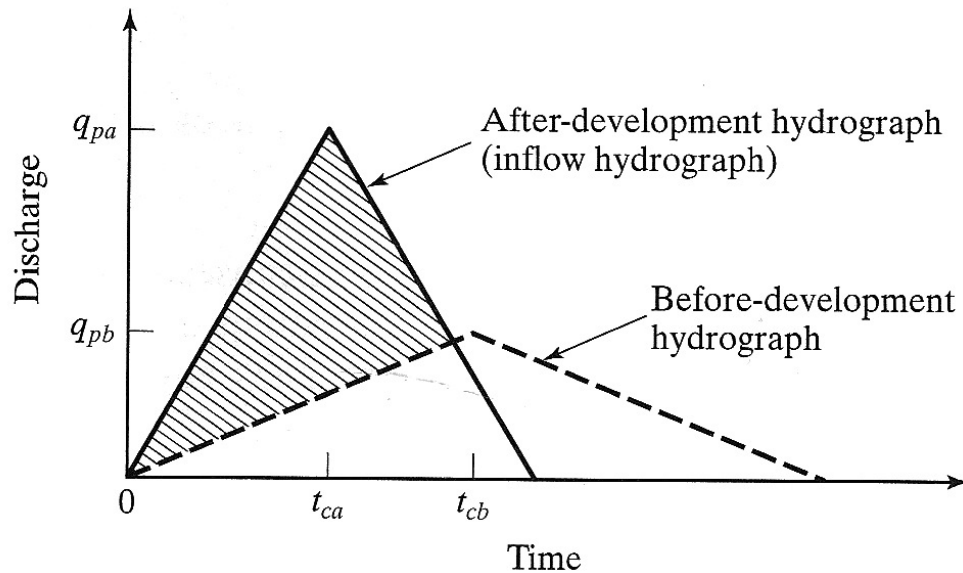


Figure 1-2 Post and pre-development hydrographs (McCuen, 2005).

Where,

q_{pa} is the peak flow rate after land development

q_{pb} is the peak flow rate before land development

t_{ca} is the time of concentration after land development

t_{cb} is the time of concentration before land development

1.2.3 Reducing the flood potentials caused by land developments.

Knowing the source of a problem is a key factor for finding its solution. As mentioned earlier, land developments came at the expense of high peak values compared with the pre-development runoff, as a result of less water storage area, less water infiltration and less surface friction.

Table 1-1 provides a list of techniques used in practice to help reduce the peak flow. When a large change in peak flow is expected, the first option an engineer should consider is designing infiltration devices (Geocellular Systems, perforated pipes, permeable surfaces) when the soil types and water quality permits, because they don't require a storage basin, which may cost a lot to build. The rate of infiltration heavily depends on the soil type: to be effective infiltration must dispose of a certain amount of the potential run-off compared to the peak flow. Areas with high levels of contamination that may risk ground water quality must avoid using infiltration devices to control the peak flow. Detention basins and other popular flow control devices will be the focus of the next section (British Water, 2005).

Measure	Advantages	Disadvantages
Cisterns and covered ponds	Alternate uses for the water stored Occupy small areas Land above has alternate uses Water conservation	Expensive to install Not large capacity Restricted maintenance access
Open space and grassed areas	Aesthetically pleasing Cost effective Pollution removal	Land availability Public acceptance problems if not well done Safety issues
Blue-green storage	Multipurpose capabilities High public acceptance Aesthetically pleasing Often cost effective	Difficulty finding suitable sites Maintenance special difficulties May be safety hazard
Rooftop ponding	Runoff delay Cooling effect on building Possible fire protection	Structural loading Clogging possibility if trees overhang Freezing problems during winter Roof leakage
Surface ponds	Ability to control large areas Can be aesthetically pleasing Multipurpose capability Aquatic habitat provider Can increase land value Pollution reduction	Requires large areas Possible pollution and eutrophication Pest breeding area Can become urban eyesore Safety hazard Maintenance problems possible
Increased roughness on roof — ripples and gravel	Runoff delay	Cost and structural loading
Porous pavement, gravel and paving blocks	Runoff reduction potential Groundwater recharge Gravel may be cheaper Pollution reduction	Cost and maintenance Clogging or earth compaction possibility Groundwater pollution Frost heave Grass and weeds grow through
Grassed channels and ditches, vegetative strips	Runoff delay Some runoff reduction Aesthetically pleasing Pollution reduction	Land loss Maintenance increase
Ponding on impervious areas	Runoff delay Pollution reduction	Restricts other uses when raining Damage due to wetness and freeze-thaw Dirt and debris collection in depressions
Infiltration devices	Runoff reduction Groundwater recharge Little evaporation loss Pollution reduction Water conservation	Clogging Initial expense Groundwater contamination
"Microlandscaping," xeriscaping, terracing, flow routing, urban forestry	Runoff reduction and delay Aesthetically pleasing Pollution reduction Water conservation	More expensive to design, construct, and maintain

Table1-1 Methods used to decrease the peak flow (Debo and Reese 2003).

1.2.4 Detention Basins

Detention basins, also called detention ponds, are one of the most popular and common flow retardation structures. Detention basins generally consist of three elements: storage, outlet and emergency spillway (see Figure 1-3). Typically, a detention pond's storages and outlets are designed to handle 2-year, 5-year or 10-year peak flow and to survive a 100-year flood when water is flowing from the emergency spillway (Debo and Reese, 2003).

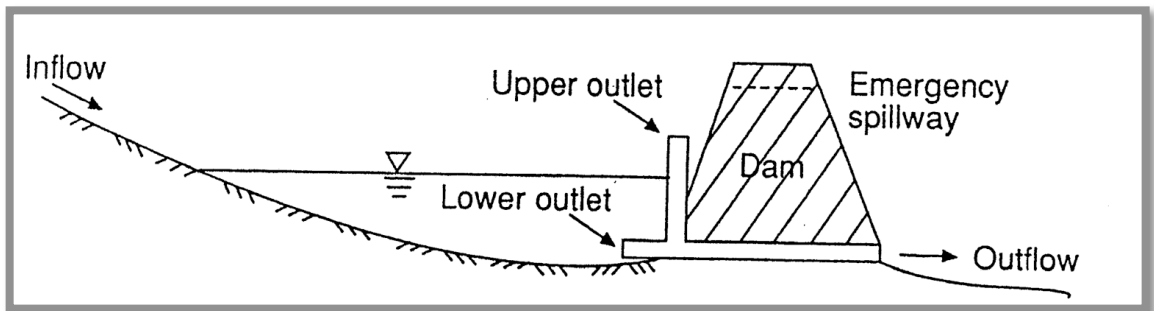


Figure 1-3 Diagram of a detention basin (Olsen, 2004).

In a rainfall event, detention basins are designed to control the outflow of the stored water so that it does not exceed the peak discharge rate for the land prior to development. Figure 1-4 shows the effectiveness of a detention basin on the peak outflow. Area A represents the storage volume needed to be stored from this rainfall event. Note in curve B, the peak outflow rate went down after passing through the detention basin. For a given rainfall event, if the inflow rate exceeds the drainage rate of a basin, the volume of the water stored will increase, demanding more storage volume. To reduce the basin storage volume, the outflow should reach its peak flow quickly and continue discharging water at the peak flow for the most discharge duration as shown

Figure 1-5. By doing so, more water volume can be drained at a shorter time period making the area above the red curve in Figure 1-5 less, compared to the whole hashed area.

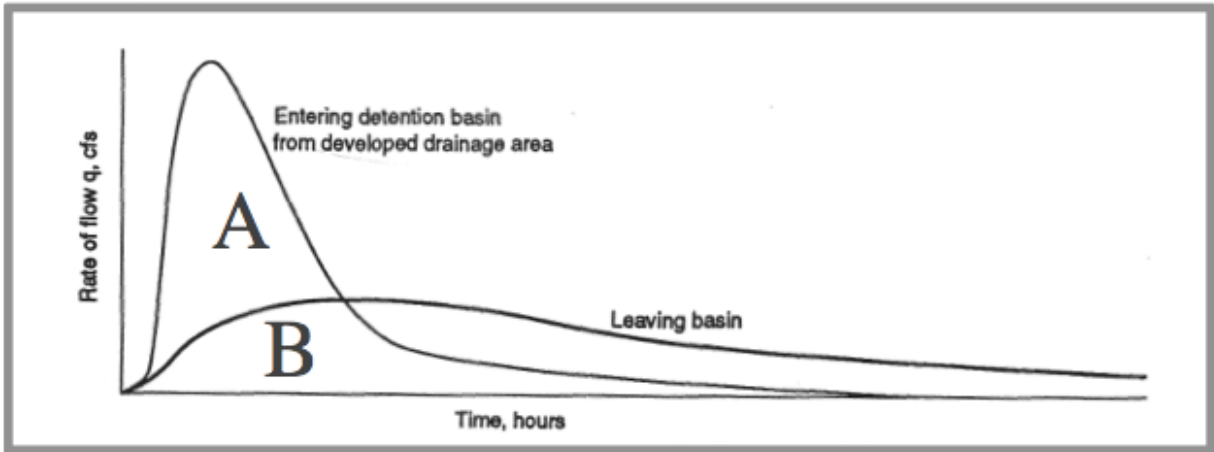


Figure 1-4 Improved developed drainage basin using detention basin (Ferguson, 1998).

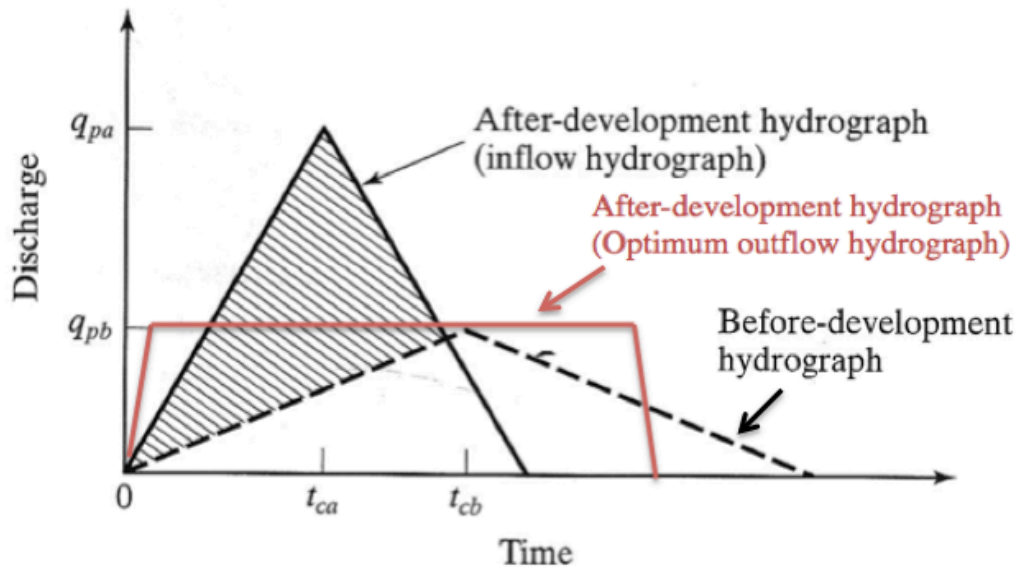


Figure 1-5 Most effective use of the detention basin storage area hydrograph (red).
 After vs before development hydrograph (Black).
 (McCuen, 2005) modified by adding the optimum outflow curve

1.2.5 Types of Detention Basins and estimating the volume of the storage area

Detention Basins can be characterized based on the stored water level (Wet or Dry), outflow discharge (controlled vs. uncontrolled) and the location of the storage (above or under the ground). Normally, land availability and cost will determine the designed storage basin characteristics. As an example, controlled discharge outflow basins are used where available storage space is limited or expensive.

Wet Detention Basins are designed to retain a certain volume of water year-round. The elevation of the outlet structure of the wet pond is above the storage area bottom or it may have no outlet structure (Retention Basins). Infiltration and evaporation are the only means that water can escape from artificial lakes or retention basins. Wet ponds will increase the water quality by allowing suspended particles to settle for a long time period (Georgia, 2001).

When the outlet structure is placed at the lowest point of the pond, the detention basins will be completely dry, as dry ponds do not have a permanent water pool. To allow sediment and pollutants to settle out, dry detention ponds are designed to detain storm water for a minimum duration of 24 hours. A pond floor slope greater than 0.5% should be designed to fully drain the flood between storm events. Semi-annual and after storm event inspections are required to ensure that the pond is fully drained from water because the wet floor is a mosquito breeding ground (South Carolina DHEC, 2005).

Detention storage can also be placed underground in areas that don't have available space for wet or dry ponds. Underground Detention Storage Basins can be designed using either underground tanks or more commonly used underground pipe storage systems with minimum diameter of 36 inches to reduce the chances of blockage

(Georgia, 2001). The drainage structure must be designed to withstand traffic loads or any applicable loads. Underground detention basins are recommended for use with other treatment controls because they don't provide any water quality treatment to storm water (ARC, 2001).

Outlet flow regulators govern the efficiency of the storage area as well as constrain the outlet flow rate. The potential energy of the stored water will be at its maximum if water reaches or is near the emergency spillway elevation making water flow at its highest rate when a basic outflow structure is in use (weir or orifice). The Energy equation (Equation 2) for fluid demonstrates this relationship by stating that the total head for a fluid for the outlet and the inlet is constant:

$$\frac{P_1}{\gamma} + \frac{V_1^2}{2g} + Z_1 = \frac{P_2}{\gamma} + \frac{V_2^2}{2g} + Z_2 + h_l = H \quad \text{Equation 2}$$

Where,

H is the total head

$\frac{P_1}{\gamma}$ is the pressure head at the upstream. (Same value as the down stream pressure head, cross out)

$\frac{V_1^2}{2g}$ is the velocity head upstream

Z_1 is the elevation head upstream

h_l is head loss

The subscript 2 is denoted to the down stream flow as shown in Figure 1-6

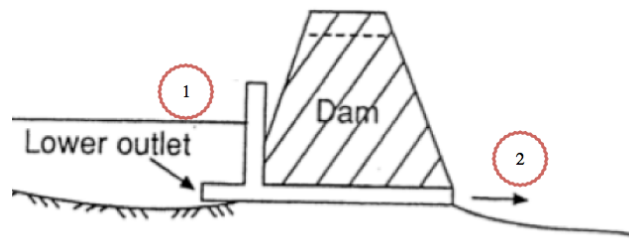


Figure 1-6 Subscript 1 and 2 in the energy equation (Olsen, 2004) modified.

Innovations have been made to provide a more uniform discharge flow rate to increase the efficiency of the storage area by releasing water at the peak flow rate. The energy equation and previous attempts suggest that constant flow rate can be achieved by (Urbonas and Stahre, 1993):

- 1- Using a device to control water head (up stream or down stream).
- 2- Using a device that changes the cross section area for the outlet or in general to control the head losses.
- 3- Using vortex to control the flow, which changes flow area and increase head losses.

The following chapter will address the innovations and inventions that have been used to maintain a uniform semi-constant flow. Developing a constant flow when the storage head varies will allow engineers to design smaller, more effective storage basins.

Chapter 2 – Literature Review for the Controlled Flow Detention Basins

2.1 Outlet Controlling Water flow Regulators

2.1.1 Orifice Plate

The orifice plate is the simplest device used to control an outlet flow rate. It consists of a thin plate that is placed perpendicular to the outlet. Water flows through a hole located in the middle of the plate as shown in Figure 2-1. As water starts to flow through the orifice, its velocity near the orifice plate increases significantly due to the restriction in the cross section area. The maximum velocity occurs past the physical orifice plate in a point called Vena Contracta. The flow rate is regulated by the minor losses associated with water exiting the orifice plate and forming large eddies. The orifice plate is an inexpensive method of controlling flow rate. However, installing this device comes with the risk of blockages due to the relatively small orifice diameter, and some concerns about the negative pressure that may also damage the pipe (Dermot, 2008).

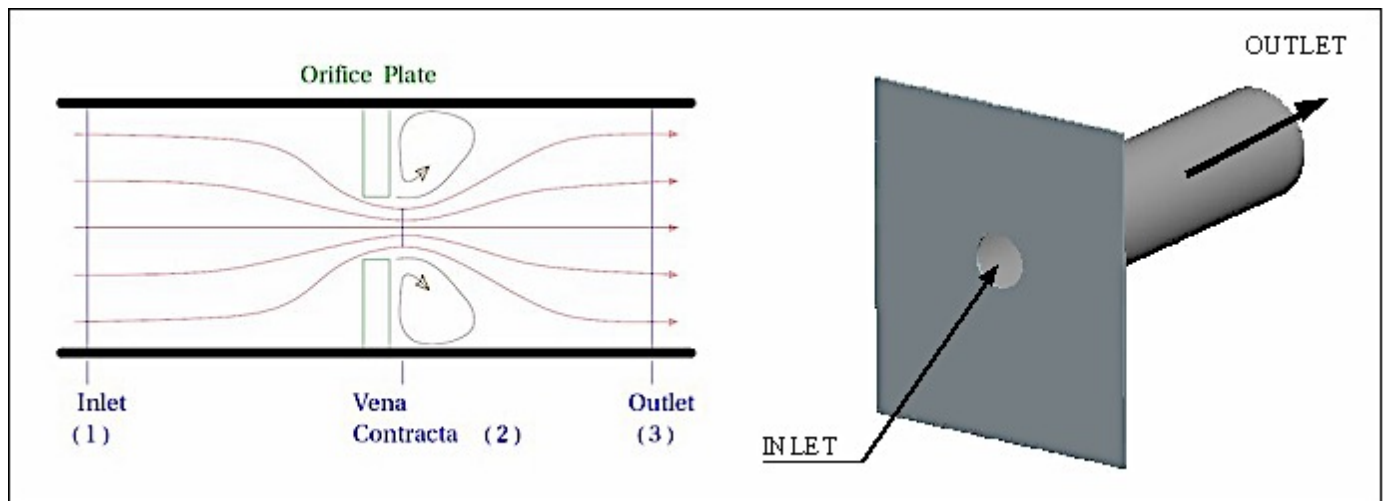


Figure 2-1 Orifice Plate configuration (Dermot, 2008).

2.1.2 STEINSCREW

A Steinscrew is a vortex storm water regulator. It uses the pipe itself as the flow-regulating device. During the designed flow the water depth inside the pipe should not exceed 75% of the diameter of the pipe. According to Urbonas and Stahre (1993), “ More depth of storage in the pipe will cause the system to surcharge frequently, which is an unacceptable design condition” (p. 183). The pipe void-volume will serve as storage for flow retardation in more extreme inflow rates. While there is no upper limit on the pipe diameter, 36 inches is the minimum recommended pipe size that uses a Steinscrew for detention purposes. Figure 2-2 shows a Steinscrew water flow regulator that consists of a twisted rectangle stainless steel plate with a width that is one-third the pipe diameter (see figure 2-2). This flow regulator device has a low maintenance requirement because its design does not consist of any movable mechanical components. The Steinscrew was tested for handling trash and debris, and was found to withstand solid wood pieces and sticks up to 4.5 feet in length, although the dimensions of the Steinscrews being tested where not discussed in the text. This device has outstanding uniform flow discharge results, especially when several Steinscrews are installed in series as shown in Figure 2-3 (Urbonas and Stahre, 1993).

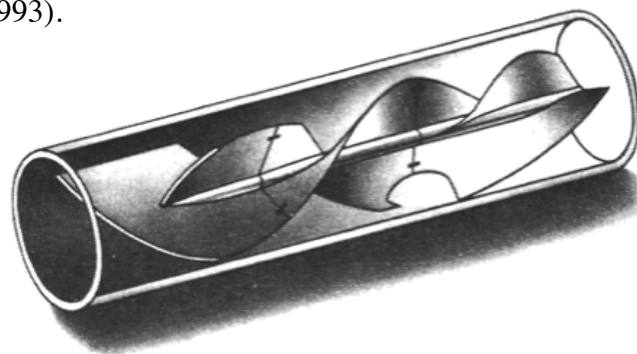


Figure 2-2 Steinscrew flow regulator (Urbonas and Stahre 1993)

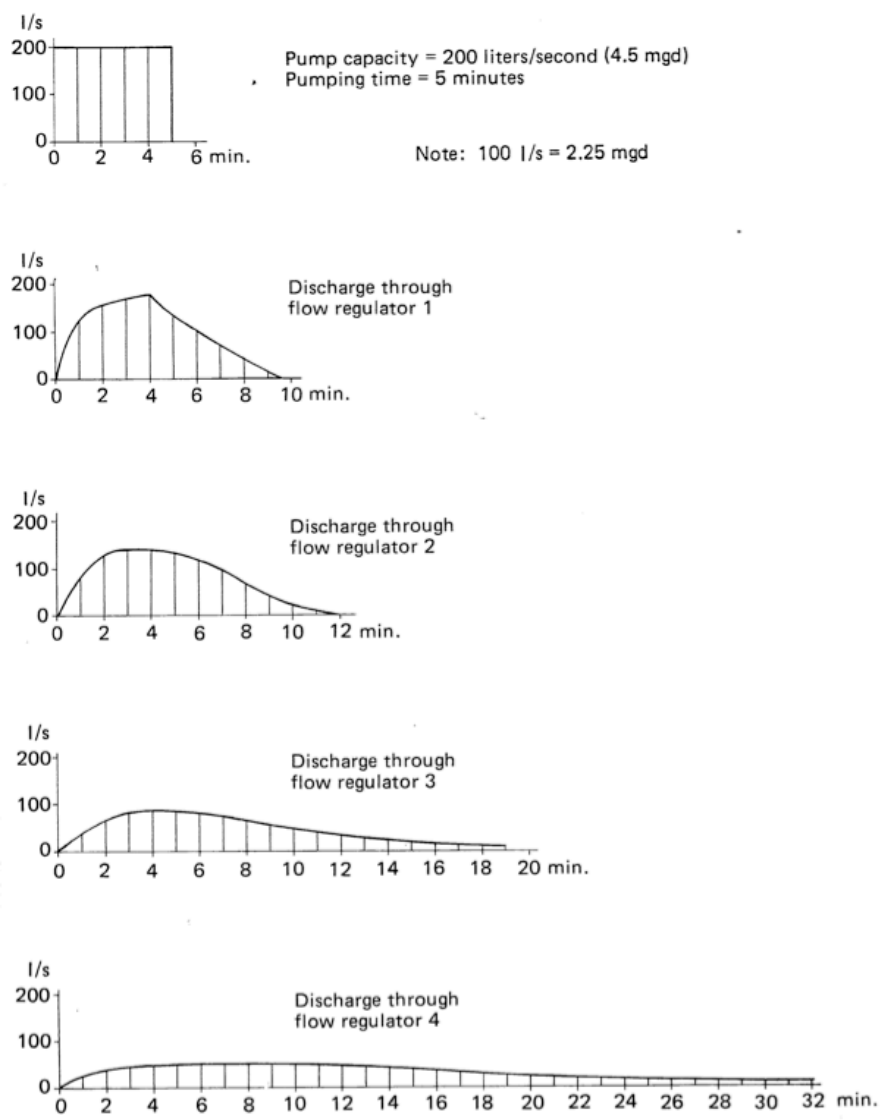


Figure 2-3 Performance of four regulators in series (Urbonas and Stahre 1993).

2.1.3 Hydro-Brake System (Vortex Valves)

Hydro-Brakes are proprietary devices that are used to control the outflow of a storage basin. The water enters the stainless steel snail shell-like frame and discharge through an orifice placed in one side of the tank frame (see Figure 2-4). At low water elevations the device acts as an orifice, providing an increased flow with any increase in the storage head. However, when the velocity reaches the maximum designed flow, water starts to spin inside the frame, creating a vortex that resists any additional increase of the outlet flow rate. Hydro-Brakes systems can deliver a more constant flow rate than an outlet operated with an orifice. Hydro-Brake devices have been used effectively to control both storm and wastewater with a low risk of clogging (Urbonas And Stahre, 1993) and (Hydro International, 2012).

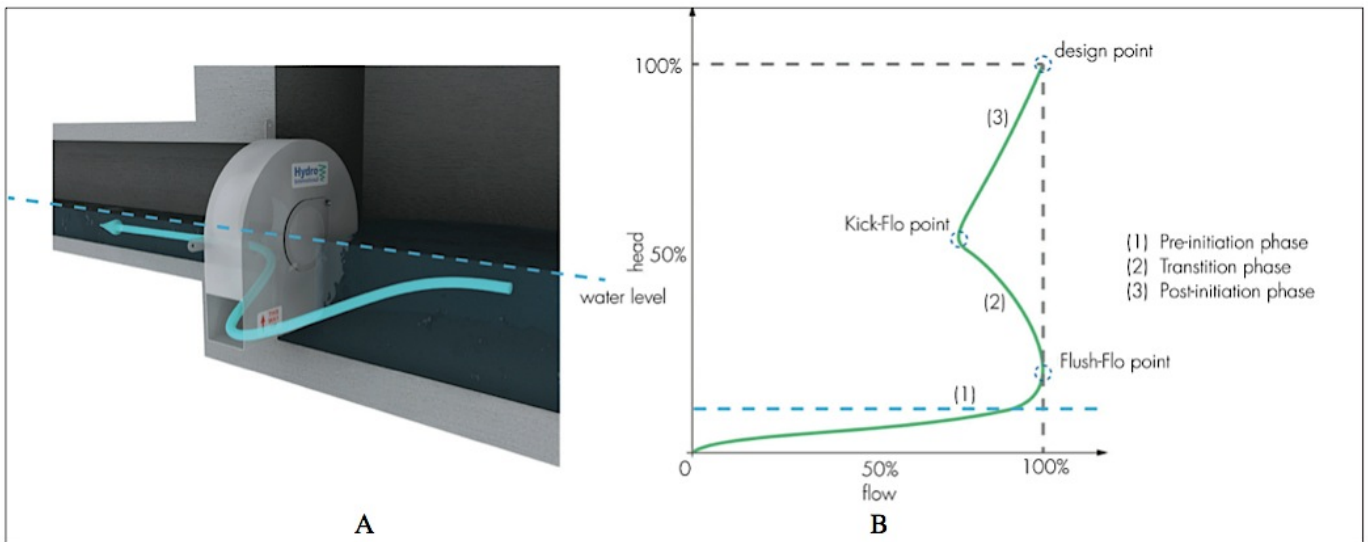


Figure 2-4 Vortex initiation phase (A). Head Versus Flow Characteristics For vortex valve controlled discharge (B) (Hydro International, 2012).

The discharge-rating curve on (Figure 2-4) highlights three important points:

1- Flush-Flo™ point:

Vortex starts to develop causing a reduction in the flow rate.

2- Kick-Flo® Point:

Vortex has fully stabilized and the flow has returned to the normal orifice-like flow-increasing rate. Flow rate continues to increase with an increase in head.

3- Design point:

The highest allowable flow rate; ideally the flow at the design point should be equal to water flow at Flush-Flo™ point. This will reduce the storage area by minimizing the peak flow of the system.

2.1.4 Wirbeldrossel and Wirbelvalve Flow regulator

A Wirbeldrossel functions very similarly to the Hydro-Brake System. It has a shallow vertical cylinder with an inlet on one side and the outlet in the center of the circular bottom plate. On the reverse side from the outlet there is an aeration pipe to help produce the vortex in the main pipe and to eliminate negative pressure (see Figure 2-5). Wirbelvalve is a modified version of the Wirbeldrossel with a cone-shaped bottom (see figure 2-5). Inspection and maintenance can be done even when the storage basin is filled with water because the device is installed in a separate sealed chamber downstream from the storage.

The geometries of the device and the positioning of the inlet pipe forces water to spin and rotate in a cylindrical tank. At higher water velocities an air pocket starts to form occupying some of the available flow. This reduces the water cross-section area flowing in the pipe, causing the flow rate to decrease. This flow regulator has passed the trash and debris test with no problems and now is frequently used in Germany and Switzerland. This device has outstanding results when it comes to flow control and has a relatively low maintenance cost (see Figure 2-6) (Urbonas and Stahre, 1993). Figure 2-6 shows that a

Wirbeldrossel flow regulator produces a relative constant discharge compared to an orifice.

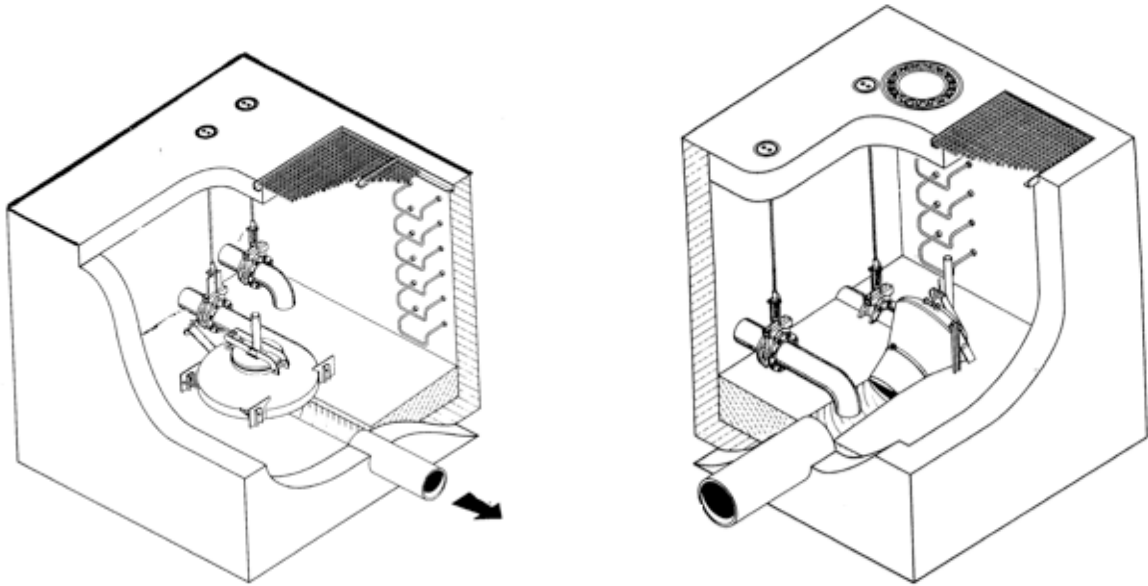


Figure 2-5 Wirbeldrossel (left) and Wirbelvalve (right) flow regulators (Urbonas and Stahre, 1993).

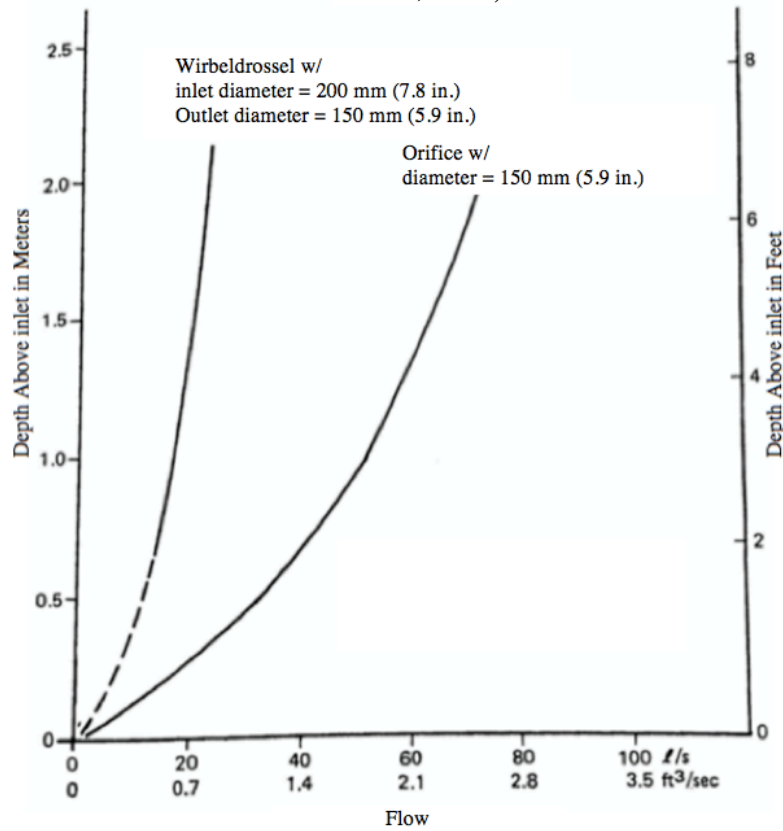


Figure 2-6 flow capacity of Wirbeldrossel vs. an orifice (Urbonas and Stahre, 1993).

2.1.5 The Flow valve

The flow valve is designed to be used in a combined sewer system to regulate the storm water and prevent it from rushing into the sewage pipe. The device can be installed easily in any circular manhole (see Figure 2-7). The flow valve looks like a hollow flange filled with pressurized air. The inside of the small cylinder of the flange and the top of the steel disc is replaced with flexible rubbery fabric. In the presence of storm water, the water head applies pressure to the top of the flexible disc, forcing it to flex downwards. Since the flange neck exerts less pressure (due to water velocity), it flexes towards its center of mass, making the flow area smaller and restricting the flow (Urbonas and Stahre, 1993). When the device was tested it maintained fairly constant flow. The Flow slowly decreased when water head increased, and over higher water heads the flow reduction was barely noticeable (see Figure 2-7). The flow regulator was not tested for trash and debris

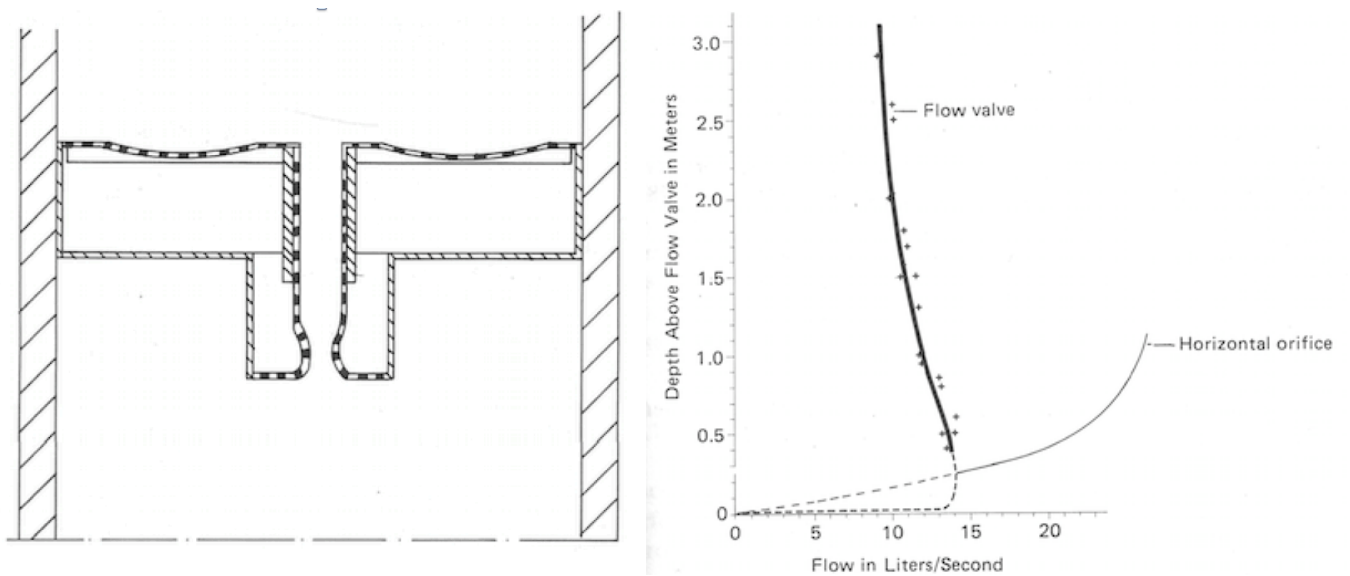


Figure 2-7 The Flow valve installed inside a manhole (Left). The discharge curve of the flow valve versus an orifice flow (Right) (Urbonas and Stahre, 1993).

2.1.6 Mechanical Floating Outlets

Mechanical floating flow regulators are designed to make the water head difference between upstream and downstream constant (see Figures 2-8 and 2-9). Either the upstream reservoir or the downstream outlet has a mechanical device, which uses floaters to lift the intake/exist pipe relative to the water head in the reservoir. If the flow regulator device uses only the storage basin water head level to control the flow, the skimmer can be blocked by tree leaves and other floating debris, forcing flow rate to diminish and water head to increase. Mechanical flow valves have movable components, which makes them expensive to operate because they require considerable maintenance (Urbonas and Stahre, 1993).

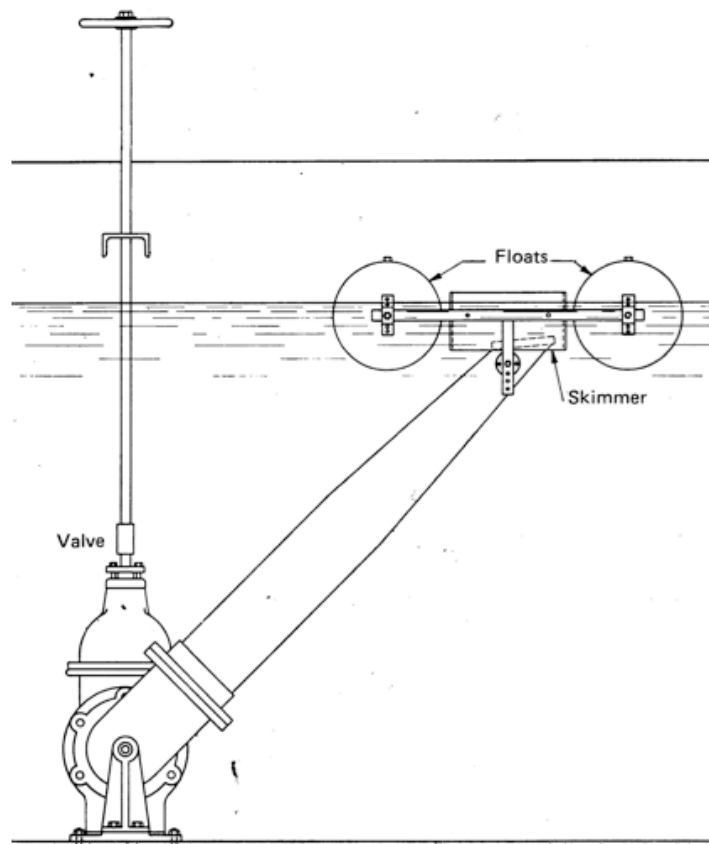


Figure 2-8 An example of floating outlet flow regulator (Urbonas and Stahre, 1993).

The device illustrated in Figure 2-8 consists of a rigid pipe attached to a valve compartment by a movable joint. The joint will give the pipe two degrees of freedom to allow the pipe to rotate around the joint. The other end of the pipe is held at a constant water depth using two floaters. A skimmer is used to filter the water entering the pipe from floating trash and debris that might cause the pipe to be plugged. This flow regulator is capable of controlling flow rates up to 2500 gallons per minute (Urbonas and Stahre, 1993). Flow graphs were not available in the text, however the flow is expected to be constant since the water depth above the device inlet is constant.

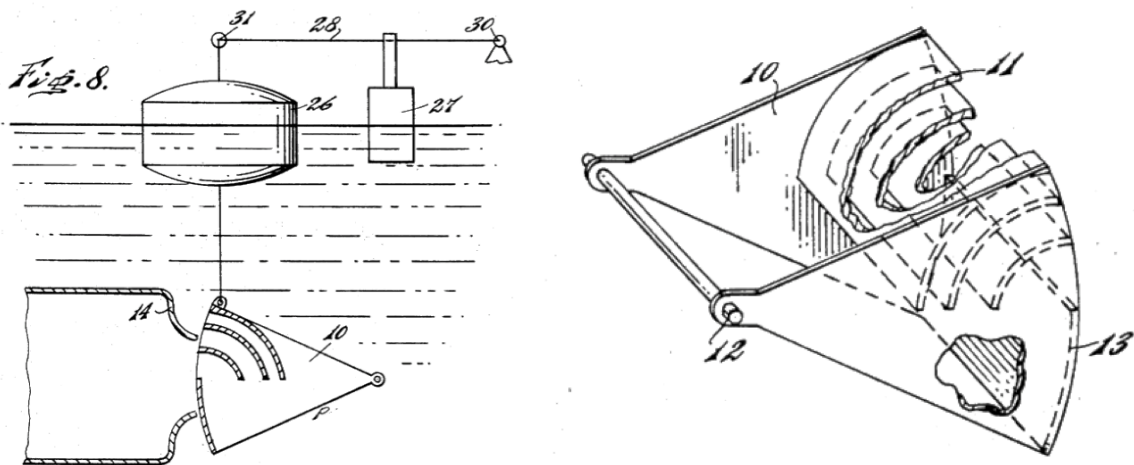


Figure 2-9 Patented self-regulating fluid flow valves (HARDY, 1968).

Figure 2-9 shows a valve that controls the flow using the buoyancy force created by the flouter. The bottoms half of the device (10) facing the outflow pipe (14) consists of flow deflectors (11) which can be designed to fit the required flow criteria and the maximum depth of the water. Just below the deflectors, a solid metal plate is placed to reduce the effective flow area when the water depth increases. The valve is designed to

never completely close (HARDY, 1968). The patent does not discuss any recorded flow data while the valve is operating.

Currently, mechanical floating outlet valves have been improved. They have fewer moving parts that come into contact with water, which reduces the maintenance cost. Figure 2.10 shows the HydrOslide flow regulator that can control flow as small as 2 L/S (0.071 cfs). The HydrOslide regulator is designed to maintain a fully open gate at the end of a storm event, reducing the risk of blockage. (HYDROK, 2014)

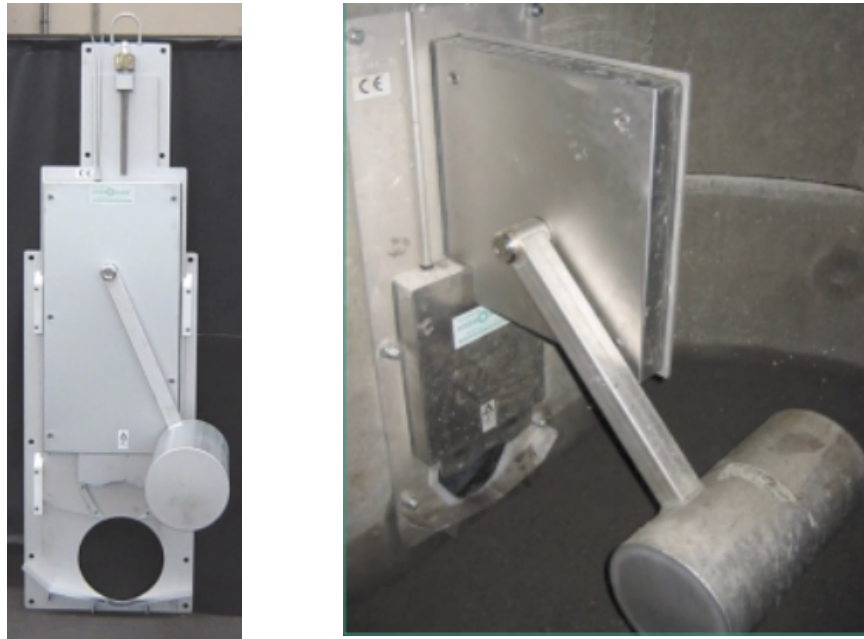


Figure 2-10 HydrOslide flow regulator (HYDROK, 2014)

2.1.7 Detention Basin Outlet Structure (DBOS)

Olsen (2004) tested a two precast concrete chambers structure that self-controls the basins outlet flow. The device, designed by Ken Gardner, is called a detention basin outlet structure (DBOS) and is shown in Figure 2-11. As the head rises in Chamber #1, a sufficient pressure will develop allowing the flow to pass through the squashed flat flexible pipe (flexible control valve) located in Chamber #2. During a storm event, water rises in Chamber #1 to reach the orifices located in the wall that separates the chambers, allowing water to flow into Chamber #2. The pressure surrounding the flexible pipe rises, restricting its cross-section area to allow a constant flow rate assuming the pressure difference inside and outside the flexible pipe is constant. The water exits Chamber #2 through a small orifice located at the chamber's bottom. If a lower flow rate is desired a steel bar can be placed under the flexible pipe to limit the maximum pipe cross-section area.

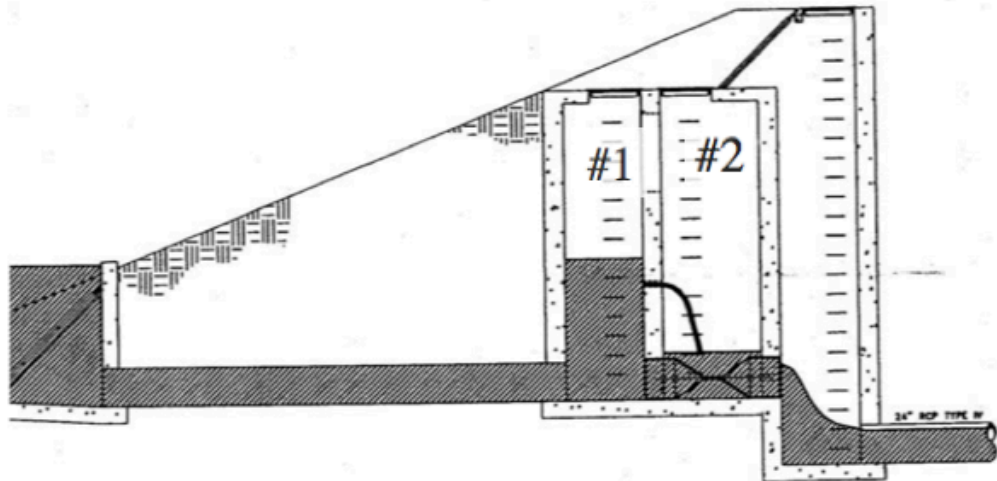


Figure 2-11 Layout of the Detention Basin Outlet Structure (Olsen, 2004).

DBOS delivered great results during the tests. In addition, it was easy to modify and reduce the maximum outflow by placing a bar under the flexible rubber pipe. Figure

2-12 shows the results of the flow tests of different head differences (H1). The device was able to produce a near constant flow when it reached its maximum designed output. However, no tests were performed to anticipate the lifespan of the outlet structure or how the outlet control structure would handle debris and trash (Olsen, 2004).

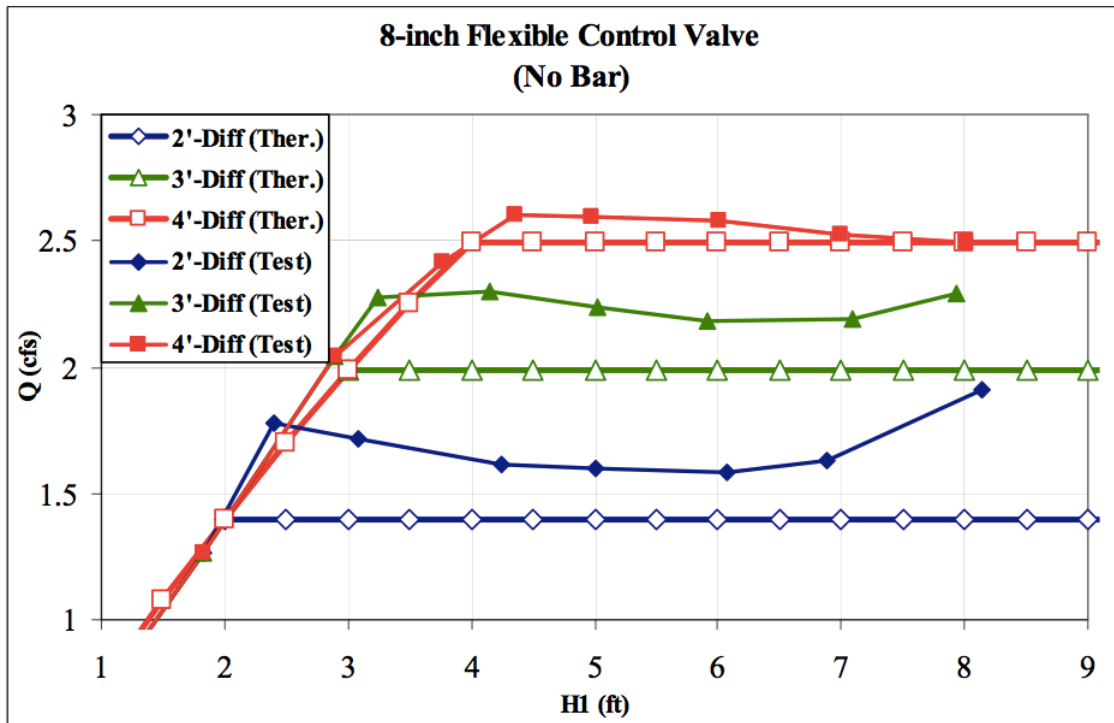


Figure 2-12 Theory vs. real model discharge flow results for the outlet structure with external (differential) pressure on the flexible gate (Olsen, 2004).

2.2 General controlled outlet design aspects and concerns

This section will be a short summary of *Stormwater Detention Outlet Control Structures*, a 1985 report. The author of this report designed a questionnaire to find out the degree of importance for each aspect of a detention pond storage area and outlet. The questionnaire focused on five design characteristics: aesthetics, hydraulic function, public safety, maintenance, and water quality. Sixty-five professionals who have a job related to designing detention ponds responded to the survey. It concludes that hydraulic function is the most important aspect in designing detention outlet flow. They ranked maintenance as the second-most important, then aesthetics, and safety. Surprisingly, the least important feature in designing water detention structures was water quality, but most of them agreed that water quality could be improved by introducing a detention pond system to developed land (Stormwater detention outlet control structures, 1985).

2.2.1 Hydraulic Function

As mentioned earlier detention ponds are designed to store water and discharge it at a slower rate. The engineer should give a great deal of attention to optimizing the pond volume by selecting the proper outlet design. The accuracy of a design is affected by three factors:

- 1) The hydrologic model used to quantify the peak flow of the water shed
- 2) The model used to estimate the storage volume of the detention
- 3) The model used to size the outlet facility

2.2.2 Water Quality Considerations

The water quality collected depends on the storage duration of the storm water. The outlet should be designed to dispose of all water in 40 hours or more. A study shows that when water is left in a stalling tube for 32 hours, more than 95% of pollutants were removed by settlement (ASCE, 1985). Vegetation around the pond would reduce the time needed for settlement. Care must be taken in regions with high pollutant rates percentage, to avoid contamination of the ground water.

2.2.3 Safety

Designers should consider the safety aspects in a project, which includes the safety of the public and the safety of the structure. The outlet structure should have no sharp edges or rocks that may harm pedestrians who are walking by. Moreover, if the dam or outlet embankment fails due to a large flood, the owner or engineer is strictly liable for all subsequent damages on the region and “Act of God” reasons is rarely considered. This places a great risk on the responsible party and means that the structure of the embankment should be designed with a factor of safety and overflow outlet to function in the event that the primary outlet fails.

2.2.4 Maintenance

Detention ponds should be designed to require the least amount of maintenance. Moveable mechanical parts that are exposed to water should be avoided because they may require a lot of attention when debris and sediment are introduced. Energy

dissipaters should be placed at the end of the outlet opening to reduce erosion. The structure should be built using non-corroding materials and should survive vandalism.

2.2.5 Aesthetics

The detention facilities do not have to look attractive but should also not be an eyesore as the minimum requirement. The designer may need to minimize the use of trash racks, which expose trash and debris, making the structure unpleasant to look at. The use of fences should also be minimizing because they might increase the curiosity of vandals. There are many ways to enhance the appearance of an outlet structure for a small amount of money, such as using colored or textured concrete. If possible, the engineer should recommend using some of the naturally available materials on the site (for example, boulders and rocks as energy dissipaters) to improve the project's appearance for low or even no cost.

Chapter 3 – Computational Fluid Dynamics

Computational Fluid Dynamics (CFD) is an approach of computing and simulating water flow behaviors using differential equations driven from the conservation laws of physics (Flow-3D, 2009). Flow-3D is commercially available CFD software used in this research to develop a flow regulator. It uses Cartesian coordinates to subdivide the domain into hexahedral cells. Average velocity and areas are stored in the center of each face of hexahedral cell, whereas scalar variables (pressure, density, total enthalpy etc.) are stored in the cell center. This technique is called staggered grid (Johnson and Savage, 2001). Conservation of mass, Newton's second law and the first law of thermodynamics are the laws of physics used in CFD to determine a fluid's behavior or motion within a specified time duration in a controlled volume (see equations 3-5). Boundary conditions are the limits, which must be satisfied at all times to solve the differential equations used in a CFD problem (Tu, Yeoh, & Liu, 2013).

3.1 Governing Equation

Flow-3D uses the general Reynolds-Averaged Navier-Stokes (RANS) and continuity equations to govern the simulated fluid behavior. Solid objects interacting with fluid in the domain are defined by the implementation of the Fractional Area/Volume Obstacle Representation (FAVOR) method. The free surface where water interacts with air is computed using a modified Volume-Of-Fluid (VOF) method (Johnson and Savage, 2001).

Fluid mass crossing a mesh grid line is conserved. Flow-3D uses the Continuity Equation used for incompressible flow with constant density governing fluid motions in the Cartesian coordinates (Flow 3D, 2009):

$$\frac{du}{dt}(uA_x) + \frac{dv}{dt}(uA_y) + \frac{dw}{dt}(uA_z) = 0 \quad \text{Equation 3}$$

Where:

u, v, w = velocities in x, y, z direction respectively

A_x, A_y, A_z = fractional area open to flow or the area open to fluid flow

t = time

Fluid flow motions are predicted in Flow-3D using momentum reduced equations also known as Reynolds-Averaged Navier-Stokes (RANS) equations. The RANS momentum equations are written as (Flow 3D, 2009):

$$\frac{dv}{dt} + \frac{1}{V_f} \left\{ uA_x \frac{du}{dx} + uA_y \frac{du}{dy} + uA_z \frac{du}{dz} \right\} = -\frac{1}{\rho} \frac{dP}{dx} + G_x + f_x \quad \text{Equation 4}$$

$$\frac{dv}{dt} + \frac{1}{V_f} \left\{ uA_x \frac{dv}{dx} + uA_y \frac{dv}{dy} + uA_z \frac{dv}{dz} \right\} = -\frac{1}{\rho} \frac{dP}{dy} + G_y + f_y \quad \text{Equation 5}$$

$$\frac{dv}{dt} + \frac{1}{V_f} \left\{ uA_x \frac{dw}{dx} + uA_y \frac{dw}{dy} + uA_z \frac{dw}{dz} \right\} = -\frac{1}{\rho} \frac{dP}{dz} + G_z + f_z \quad \text{Equation 6}$$

Where:

P = pressure in the fluid

G_x, G_y, G_z = body accelerations on the fluid

f_x, f_y, f_z = viscous accelerations of the fluid

V_F = the volumetric flow rate

ρ = density of the fluid

Flow-3D uses the Fractional Area/Volume Obstacle Representation (FAVOR) technique to describe a solid object inside a meshed domain. It gives a value of one for cells that are fully occupied with the object mass, zero for cells that are not related to the object and a value between zero and one for cells that are partially occupied with objects based on the solid volume percentage. A first order approximation with a straight line in two dimensions and plane in three dimensions is used to determine the surface shape of solid objects interacting with the fluid. FAVOR is an effective tool to approximate the curves of a surface but it is still an approximation of the surface (Johnson and Savage, 2001).

Flow-3D uses similar approach to FAVOR to determine the volume of fluid in each cell called Volume-Of-Fluid (VOF) technique. Cells' occupancy with fluid is evaluated as: fully occupied cells with fluid are assigned with value of one, cells with no fluid are assigned value zero and value assigned between zero and one for partially occupied cell based on fluid percentage in the cell. Fluid slope within the partially occupied cells is calculated considering an algorithm that uses the surrounding cells based on its interaction with the fluid. VOF allows fluid geometric criteria in a cell to change over time and space (Johnson and Savage, 2001).

3.2 Numerical Approximations

FLOW-3D uses the Finite Difference method (FD) and Finite Volume approximation (FV) to discretize the fluid dynamics governing equations (Euler and Navier-Stokes). General Moving Objects (GMO) technique is used to simulate the interaction between solid objects and fluid flow. Flow-3D has many other useful physics

equations that are not used in this research such as Finite Element Method (FE), which is used to simulate deformation on a solid component due to stress exerted by its interaction with fluid. (FLOW-3D, 2009)

The finite difference method is used to provide a simple discrete algebraic equation for a partial differential equation. It uses the Taylor series expansion to generate finite difference approximations for the fluid dynamics equations. This method will approximate the solution for the governing equations and calculate its approximate solution for each grid point. The finite difference method can be applied to any type of grid. However, to maintain high accuracy, it is typical to apply FD on a uniform grid system. (Tu, Yeoh and Liu, 2013)

Finite Volume method is the most popular method used by commercial CFD softwares to discretize the Euler and Navier-Stokes equations. It is popular due to the lack of restrictions on using unstructured mesh grid, and it does not require transformation of equations to the local coordination. The application of FV method starts with dividing the domain into a finite number of control volumes. Interpolation is used in each cell to estimate its average variable dynamic properties. These dynamic properties are then evaluated using the conservation of energy method as fluxes at the surfaces of each finite volume. (Tu, Yeoh and Liu, 2013)

A General moving object (GMO) object is defined as a rigid object with 1 degree of freedom or more. Flow-3D uses GMO to simulate the dynamics interaction of a rigid object with the fluid. The motion of an object can either be user-prescribed or dynamically coupled with the fluid interaction. The GMO physics has a collision model to simulate the collision response of the two objects. The collision model can be turned

off which will allow two or more solid objects to overlap without any dynamic interference on the other object. This is physically impossible using today's technology but it is very handy for the proposed device as discussed in the chapter 4.

3.3 Meshing

CFD software analyzes fluid flow across a flow domain or control volume by using a mesh, which is a network of computational cells that are grouped together. The number of cells in a mesh represents the resolution of the simulation; the minimum size is usually limited by the computational performance of a computer. In other words, using a smaller grid mesh can yield more accurate results but will require more computational time to calculate the governing equations across the mesh. One can conclude that the face surfaces of an object in the controlled volume with more fine details will require more mesh cells to calculate the effects of the fine curves and angles on the flow.

FLOW-3D uses hexagonal or cuboid grids for meshing the control volume because they are easy to generate and require small amounts of computer storage. Curved obstacles interacting with the fluid in the controlled volume will yield many blocked mesh cells which are meant to only be partially occupied by the object volume, causing undesirable fluid motion effects. The Fractional Area-Volume Obstacle Representation (FAVOR), option is used by FLOW-3D to create more realistic simulation and eliminate undesirable fluid flow effects by resolving several geometric issues when the 3D obstacle drawing interacts with the mesh. The FAVORize view enables users to diagnose the model built using the specified mesh and to repair it before running the simulation. The defective model can be repaired either by using a finer mesh grid near the defected area

or by changing the minimum percentage for the occupied cell to be filled with the object volume (Flow3D, 2009).

Chapter 4 – Methods

4.1 Mechanical Floating Outlet device

When the hydraulic head at the storage reservoir increases due to a storm event, the outflow of the storage should not exceed the pre-development peak flow (see section 1.2.2). Outflow should stay at the peak flow to minimize the area needed for the storage basin (see section 1.2.4). Outflow will stay constant if the difference in the hydraulic head between the storage reservoir and the outlet is constant, as shown by the energy equation (Equation 2). In other words, if the outflow pipe moves vertically and synchronizes with the reservoir head keeping a constant distance between the hydraulic head in each one of them, the outflow will stay constant.

The proposed device for regulating the outflow consists of a vertical pipe/hose that can be raised using the buoyancy force. The flow regulator is located at the downstream side of the embankment, and floaters are placed on the top and inside of the pipe to provide enough force to lift the vertical pipe/hose to allow water to flow from the slots as shown in Figure 4-1. The buoyance force is provided from the water inside the pipe. The goal is for the device to maintain a constant submersion volume of the floater, causing the flow over the slots to be constant, assuming that the weight of the pipe is constant and there is no other downward force present. Having the water inside the pipe control the outflow has the advantage of more steady flow, because flow is not effected by the storage surface water waves.

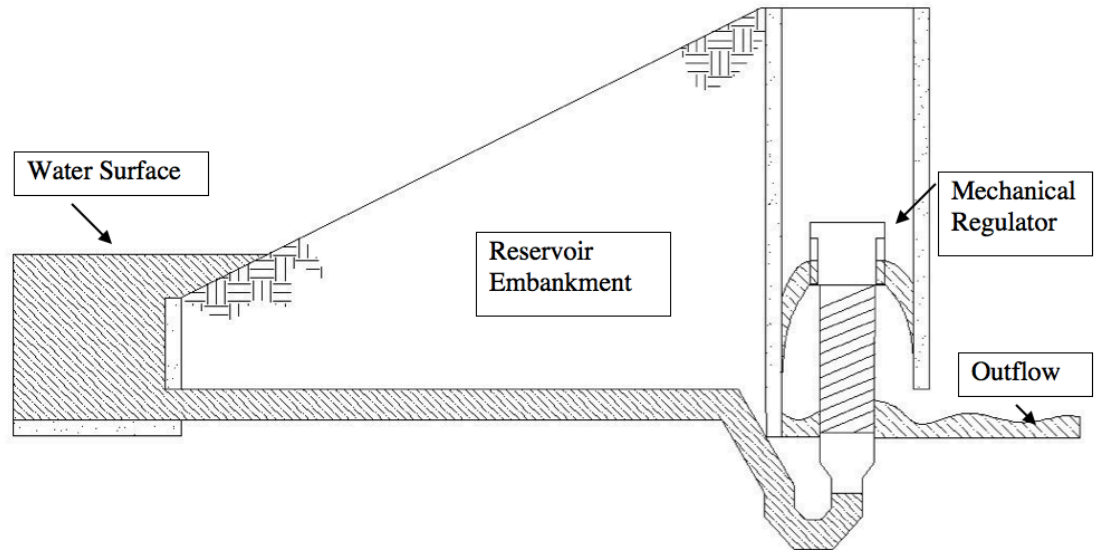


Figure 4-1 Schematic drawing of the regulator location.

A series of Flow-3D simulations were used to determine the validity of the flow regulator concept design. The Archimedes' principle for buoyancy was used to determine the volume needed for the partially submerged Styrofoam floater. A 3D drawing of the physical project layout was developed using *SolidWorks* after the hydraulic design was fully developed. The goal of having the 3D drawings is to accelerate the process of assembling the physical model. The 3D drawings help in reviewing the model and purchasing the expected quantity of materials and in producing a good estimate for the project's cost. The physical model was then built to conform the physical data to the CFD model. It also provided construction experience (such scheduling, construction time, and managing the project) and how the model would interact with less ideal environments when friction is introduced.

4.1.1 Flow-3D models

Flow-3D was used to predict the movements of the floating outlet pipe and insure the validity of the concept. It also provided water flow data, which can be compared against mathematical equations (Appendix A) and against the physical model. Vertical buoyant rising outflow pipe is a hard concept to simulate using CFD software. Flow-3D uses General Moving Objects (GMO) physics to simulate the movements floating objects. One challenge with Flow-3D's GMO method is the object must be rigid (can't expand) and be drawn inside the control volume, which will add one more degree of difficulty to the simulation setup. On the other hand, Solid Objects volume overlapping is allowed but if it is used at time step zero, it will cause a tremendous increase in the time of each step the simulation takes, which may cause the simulation to crash. In the next subsection, simulation attempts and results will be discussed.

4.1.1.1 General Moving Objects overlapping at time step zero

Flow-3D's implicit general moving objects physics was used to capture the motion of a low-density ($\rho = 0.01 \frac{\text{slug}}{\text{ft}^3}$) moving pipe under upward lift buoyancy force. The floating pipe's outside diameter measured at 9.36 inches and had 2.16 inches of wall thickness. The pipe extends 1.5 feet vertically, starting one foot away from the bottom of the controlled volume boundary. A cylindrical gap was inserted at 0.5 feet from the top of the pipe. The cylindrical wall, around the gap, thickness is 0.6 inches; just enough for the mesh to capture the curvature of the object without introducing defects when 0.3 cell sized mesh is used. Water flow into the pipe fills the gap creating upward pressure (buoyancy pressure) to push the volume of the Styrofoam on top of the gap; making the

top part of the pipe behave as a floater. The pipe was topped with a heavy cylindrical weight component ($\rho = 2.563 \frac{\text{slug}}{\text{ft}^3}$) to keep the floater partially submerged. The density of the cylindrical weight component was calculated using Archimedes' Law of Buoyancy (See Appendix A for calculations).

Another fixed object was added to the simulation's geometric design, to guide the water, which enters the controlled volume. The fixed object consists of a solid component that blocks cells and is within two feet of the bottom boundary and also has a thin wall covering the right boundary. Water enters the control volume through a 0.6 X 0.8 square foot hole on the bottom of the wall. The hole extends to the right through the fixed object until it meets the other circular vertical hole that goes through the object. The vertical hole has the same inside diameter as the floating pipe (see figure 3-2).

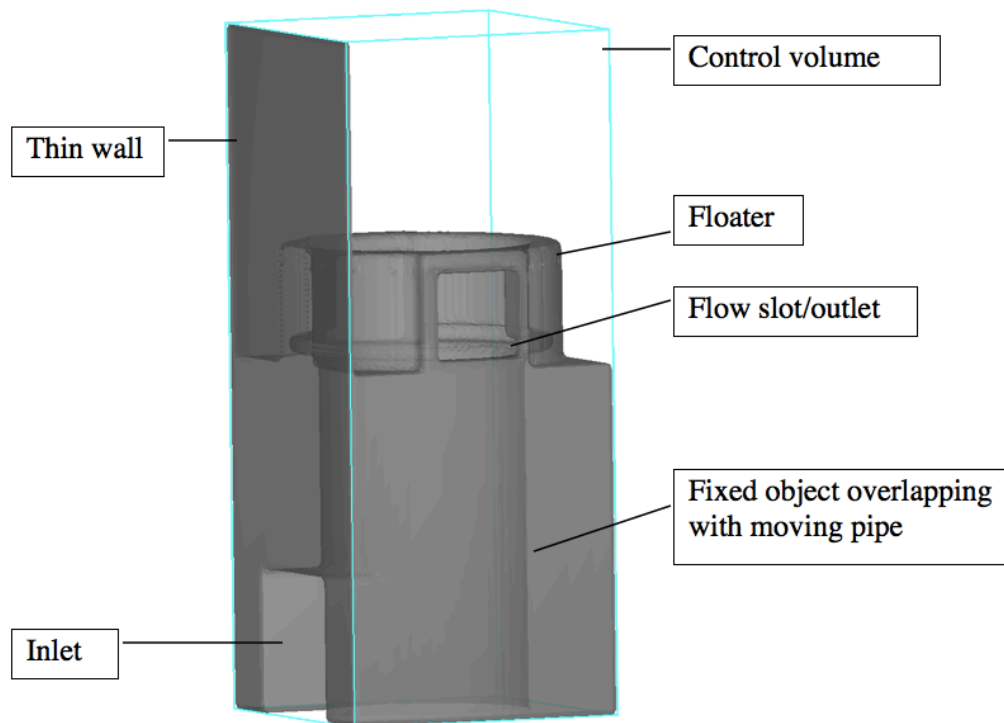


Figure 4-2 Transparent FAVOR view of the solid object inside the controlled volume (blue lines)

It is important to note that, when the simulation was running, there was no buoyancy effect from the pipe section under the gap and this could be explained using the Archimedes' principle of buoyancy. The Archimedes principle states that a submerged body in fluid will exert upward force equal to the submerged volume of the object multiplied by fluid density. The buoyancy force is exerted from the pressure difference between the top part of the object and its bottom. However, the simulation was set to have no water partials under the moving pipe, therefore the only vertical pressure it will have will come from the floater.

The pipe was set as the moving component in the simulation and surrounded by a 2-foot deep fixed floor, that has a 7.2 inches circular hole of the same diameter as the inside diameter of the pipe. The pipe thickness and the deep floor areas overlap, to ensure that there will be no water particles under the moving pipe and to maintain the same inside diameter of the pipe as it moves up. Flow-3D will allow objects to go through each other with no resisting forces (moment and friction) as long as the collision model is not activated. However, starting at time step zero with an overlapping general moving object will cause stability problems when running the simulation (J. Burnham, 2014). The simulation step's size was only controlled by stability, without convergence, so it does not crash. If the convergence and the viscosity physics setting are turning off, the simulated outflow rate will be less accurate but the simulation time will be significantly reduce. Note that the goal of this simulation is to see if it is possible to make a pipe float using the fluid inside it and predict potential problems.

Water will enter the pipe from a square opening placed on the floor's left side bottom, because Flow-3D restricts the water flow entering the control volume controlled

by elevation not to be used along the gravitational force orientation. Furthermore, water entering the pipe from the bottom controlled by variable pressure ($h = \frac{P}{\gamma}$) parallel to the gravitational force direction will cause a tremendous reduction in the time steps, caused by the software adjusting the pressure while the object moves upward and while water is flowing out of the slots.

At the right mesh boundary, the assigned starting water elevation at time zero was 1.9 feet and increased incrementally to reach 2.8 feet at 90 seconds and kept at that elevation for the rest of the simulation. The pipe moved upward as the water elevation increased but the water depth above the slot held constant. . The pipe was only allowed to move along the positive vertical direction. The weight of all the moving components and the buoyancy force coming from the pipe (density above the gap) are the only forces acting on the moving pipe. The water discharge stayed relatively constant with a little bit of fluctuation caused by the way Flow-3D handles elevation increments (see Figures 4-2 and 4-3). The simulation showed that it is possible to synchronize the pipe height with the reservoir head using the buoyancy force from water inside the pipe.

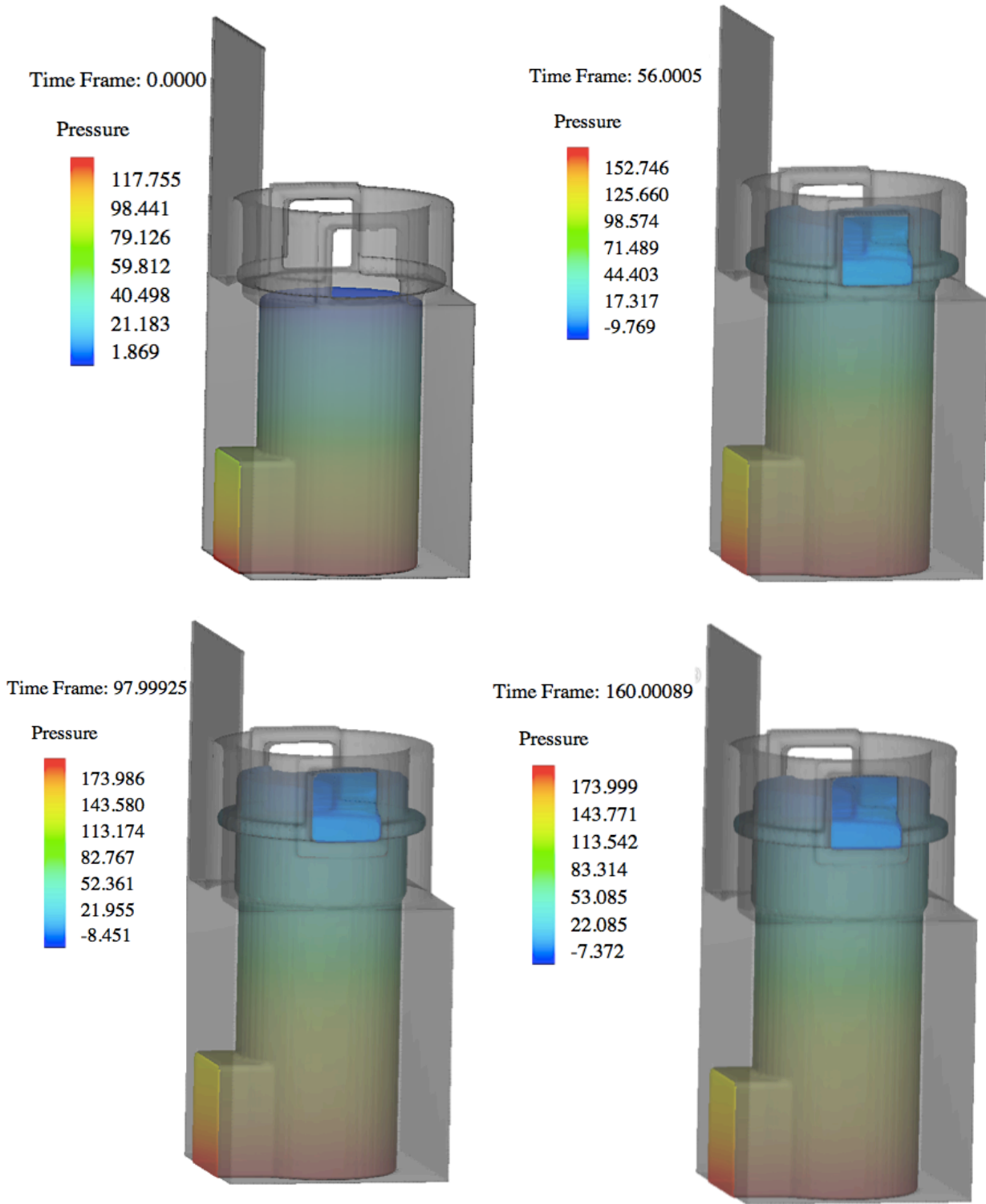


Figure 4-2 Different time step for General moving objects overlapping at time step zero After water reached a certain elevation (at 56 sec) the water depth above the slate opening stayed constant.

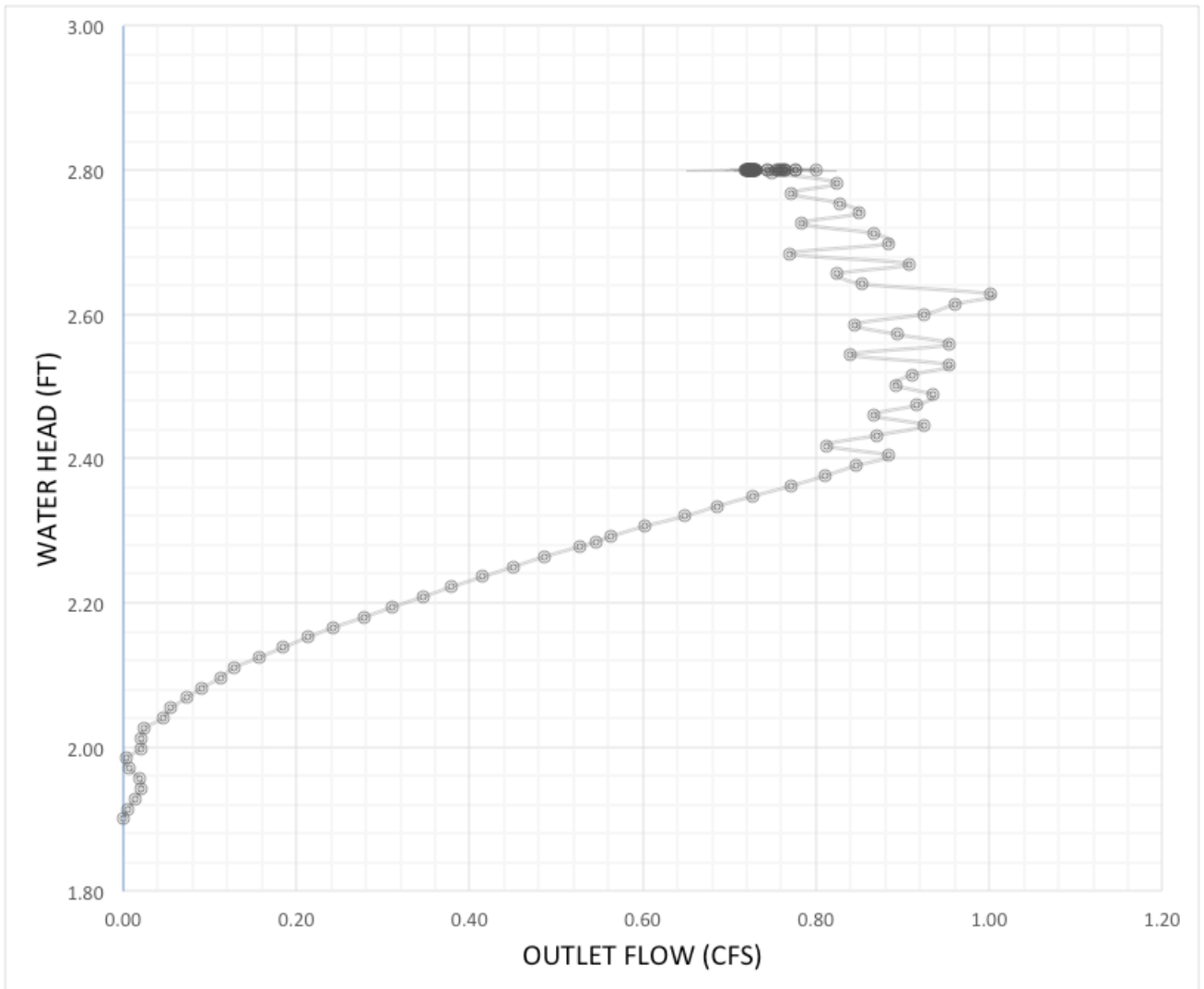


Figure 4-3 Operating flow over variable head using General Moving Objects overlapping at time step zero simulation

The water hydraulic head inside the pipe is designed to increase at a rate of one foot every 100 seconds. In theory the outflow should increase, covering more volume of the submerged floater until the buoyancy force of the floater has enough force to lift the moving pipe (Figure 4-2). The pipe will rise to keep a semi constant effective cross-section area at the slot, which will restrict the flow. Small oscillations are predicted to occur due to the downward pipe mass acceleration force when it moves ($\sum F = M \times a$).

Figure 4-3 shows a small reduction of the flow after the float is rising. It is expected that the small reduction of the flow is due to the way FLOW-3D handles the density of the overlapping objects. FLOW-3D will assign the density of the overlapped section equal to the first component in the Geometry tree (J. Burnham, 2014). In this simulation, the first component was the fixed floor (zero density) so the flow is expected to increase over time, and not decrease, because the fixed object weight is less than the moving pipe. Therefore, the pipe will be slightly heavier as it moves upward allowing more water flow to pass through the slots. However, the simulation flow chart showed the opposite effect. It is also possible that the flow reduction is due to the weirs discharge coefficient, which tends to reduce the flow as the structure under the weir is built higher. This coefficient will be discussed in more depth in the results chapter.

4.1.1.2 General Moving Objects with No Overlapping at Time Step Zero

This was an unsuccessful attempt to resolve the error messages in the previous simulations. The overlapping volume of the moving object at time step zero caused the simulation time step to dramatically reduce. The idea was to extend the control volume 4 feet downward and let the moving pipe float on the water under the rigid floor before it overlaps with the GMO. The simulation calculations went smoothly with longer time steps and no error messages as the pipe moved up through the rigid floor. Error messages “pressure iteration did not converge” started to appear when the pipe bottom was completely inside the nonmoving component. To avoid crashing the simulation at that time, stability was set at unity to control the time steps (without convergence). At that time no water particles were present under the pipe, however the pipe kept rising even

before water reached the floater (see figure 4-4 and 4-5). This means that the simulation is breaking the Archimedes principle for buoyancy because there was no water under the pipe to provide the upward pressure force. The outflow stayed at zero for all of the simulation time steps.

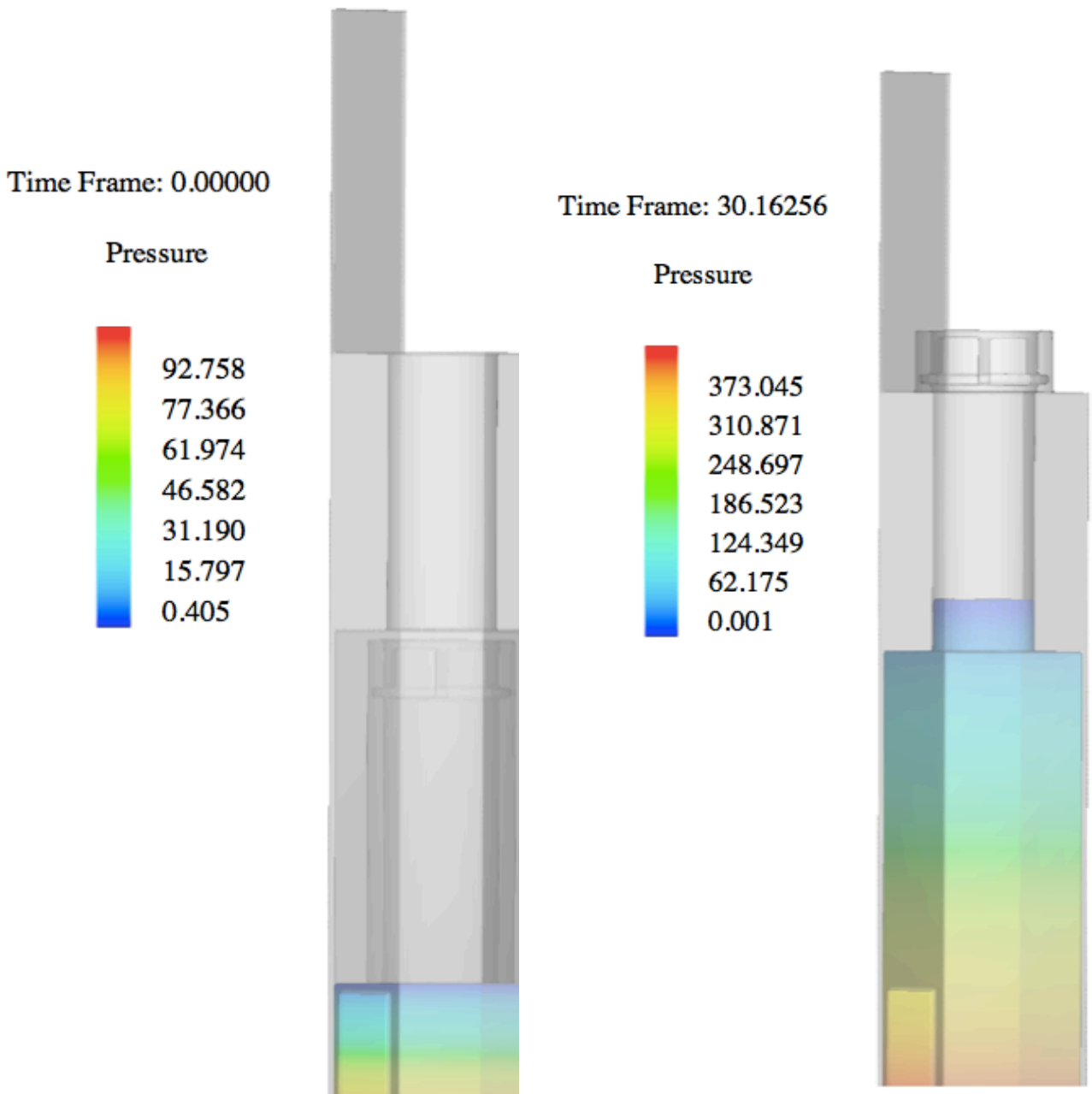


Figure 4-4 The initial time frames of no overlapping GMO simulation shows the moving pipe kept rising through the rigid floor

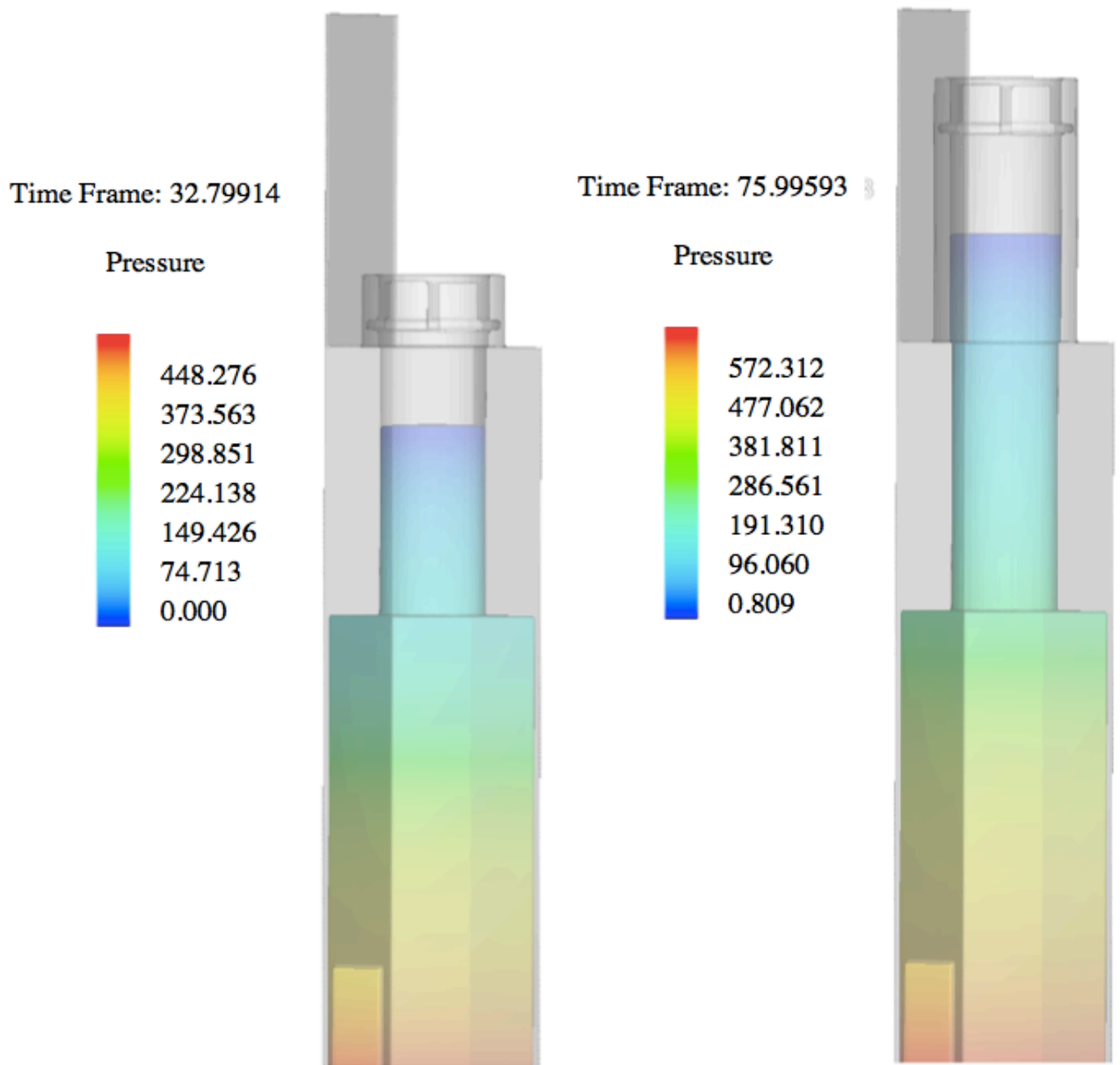


Figure 4-5 Advance time frames of no overlapping GMO simulation shows the physically impossible behavior of the moving pipe.

4.1.1.3 Series of Simulation General Moving Objects with Physics Turned off with Different Incremental Hydraulic Head and Pipe Height.

Another 3D simulation was developed with the general moving object model turned off. The second-order momentum and the viscosity model were turned on to create a more realistic estimation for the water flow. The viscosity model will simulate small eddies and shear friction between the water particles which will slightly reduce the overall outflow. In this simulation the pipe height was fixed. The simulation was copied and run at different pipe heights. The hydraulic head was adjusted to keep a constant difference between the pipe slot and the hydraulic head, because this is how the physical model is expected to behave. These simulations will be used to compare the flow in the vertical pipe to the rectangular sharp crested weirs equation when the flow is horizontal or when it is vertical.

Initially, it is expected that the water flow will increase until the buoyancy force is strong enough to lift the pipe illustrated in Figure 4-7 at a water depth of approximately 1.3 feet. In this particular simulation the depth of the water above the slot was assumed to be 0.3 feet, when the buoyance force lifts the pipe. This setup allows the flow to be compared with the previous simulations. Assuming that the weight of the pipe is constant, no friction and that there is no acceleration force, the difference of the hydraulic head between the reservoir and the slot will stay constant. If no additional buoyance force is needed to lift the pipe the water depth above the slot will stay constant making the outflow constant. This means that water depth above the slot should stay constant as the pipe moves upward if the all-vertical forces are constant making water discharge constant too. The water depth above the slot will stay constant as the pipe height rises, resisting

the change in the hydraulic head at the reservoir until the pipe reaches its limit and cannot move up any more. When the pipe cannot move upwards any farther the flow will start to increase.

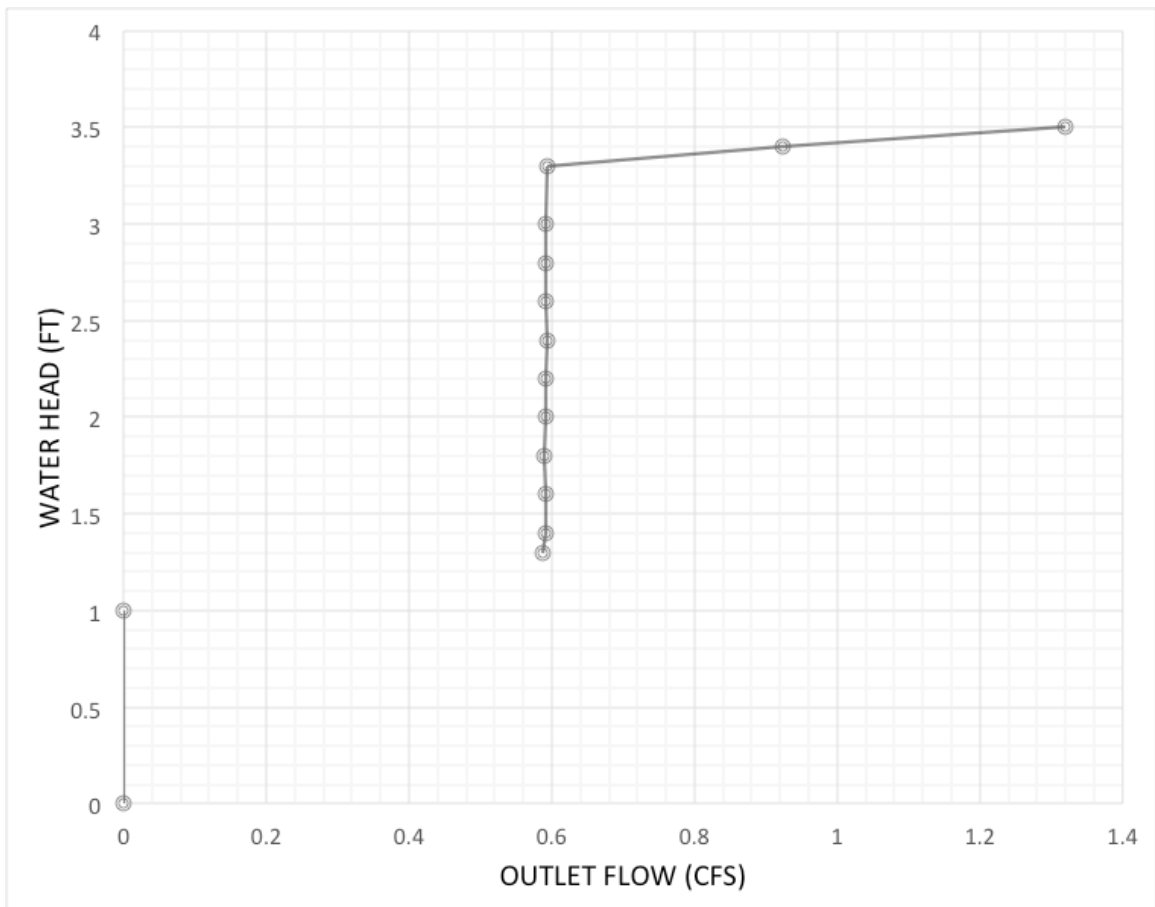


Figure 4-6 Series of stabilized flow simulations at different fixed pipe heads and their predicted hydraulic head output

4.1.2 Physical Model

The FLOW-3D model showed the possibility to develop a nearly constant flow discharge using a floating outlet pipe moving vertically, within the constraints of the model. Two methods to raise the outlet pipe were considered in the initial development stage:

1-Telescopic pipes layout: Using three rigid pipes with different diameters placed vertically inside each other. The pipe with the biggest diameter and also the longest has a floater attached to it. Water will flow out of the regulator through slots placed on the outer pipe (See Figure 4-7).

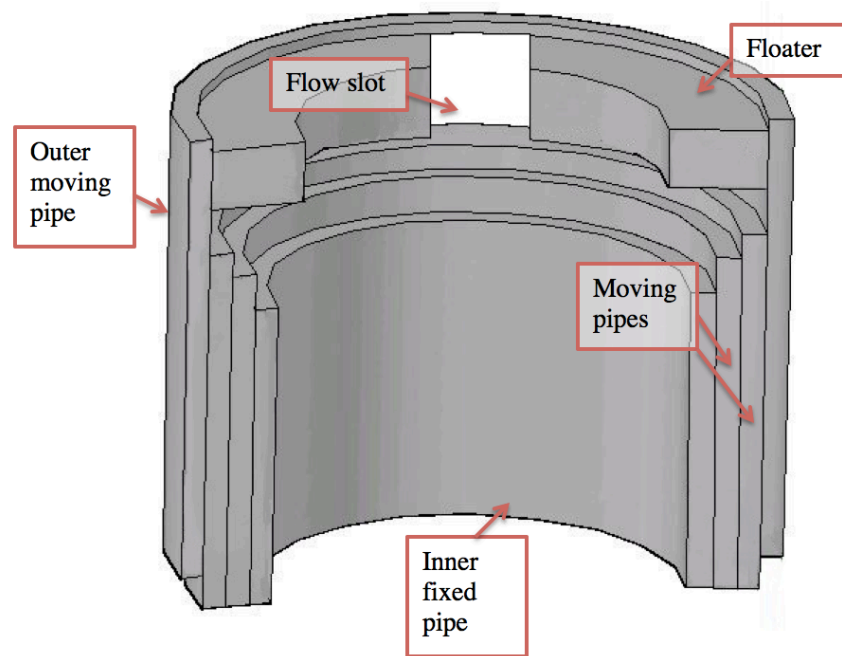


Figure 4-7 Vertical cross section of the telescopic pipes layout.

2- Flexible Hose: Using a flexible hose that can collapse to a smaller height. The hose has to return to its collapsed shape easily. A hose with a big extension ratio is preferred to provide more range of flow control.

The telescopic pipe option was ruled out due to the high potential of leakage and static friction between the pipes and the gaskets. On the other hand, the flexible hose option will introduce a twisting motion and downward force (due to the spring's shape), which will be counted for in the design (see Figure 4-8).

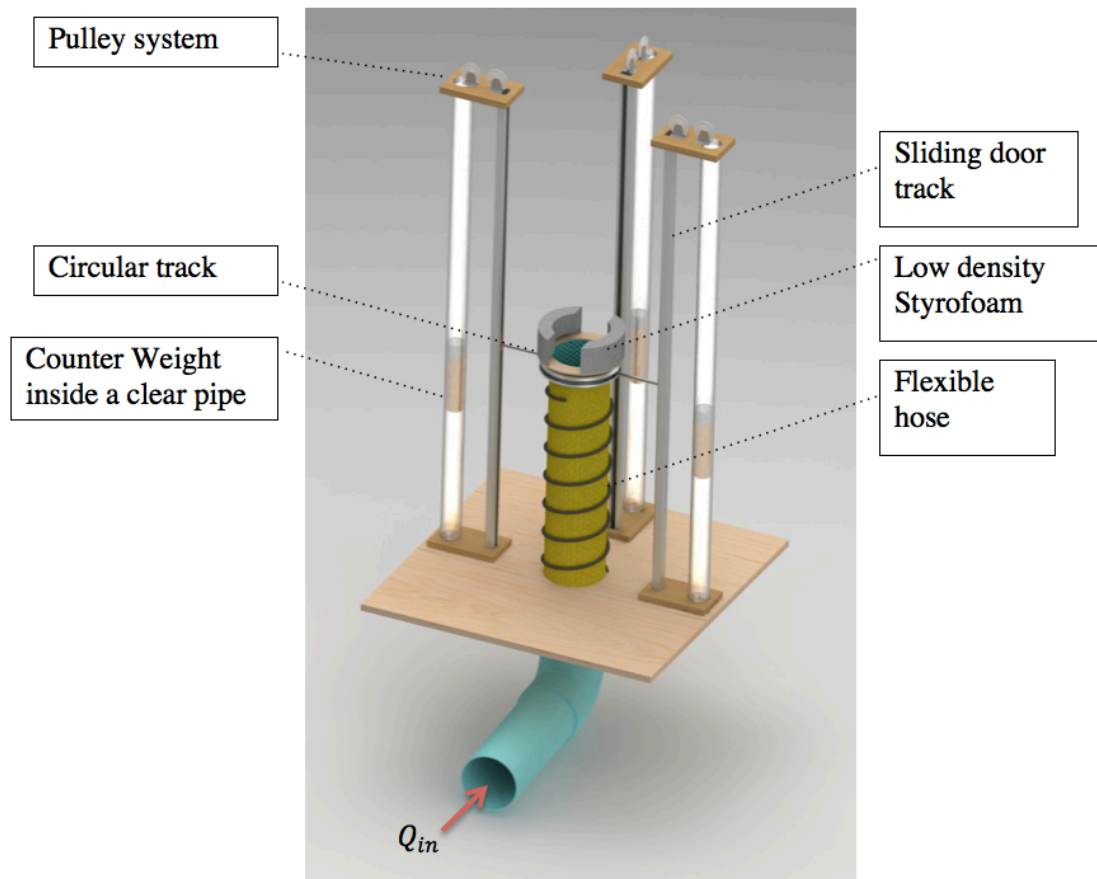


Figure 4-8 3D SolidWorks, 360 Photoview. The proposed flow regulator.

4.1.2.1 Physical Model Concept

As shown in Figure 4-8, the SolidWorks model consists of a flexible 8-inch diameter hose that has a spring wire wrapped around it to ensure the hose does not bulge out due to the water pressure inside the hose. On the top of the hose is a low-density Styrofoam cylinder with two rectangular slots cut out of it to allow water flow out of the regulator. The inside diameter of Styrofoam is the same size as the inside pipe diameter (8-inch) to ensure that the uplift of the hose is coming from the buoyancy not from the pressure created by the water velocity. The wall thickness of the Styrofoam is 4 inches, with a thin gap under it providing 0.968 pounds for every vertical inch of water depth that is submerged with the slots width as 3 inches (See Appendix B for calculations). Under the floater there is a 1-inch high gap where a thin wall supports the floater. As discussed earlier, a small gap between the Styrofoam cylinder and the hose is needed to allow the water to push the low-density floater upward. The hose is connected to three sliding tracks mounted around the hose on the base. The tracks are attached to the hose with a circular track that allows the host to rotate as it moves vertically but restrain the motion horizontally. A pulley system is attached to each one of the slides to counter the weight of the moving components of the hose.

4.1.2.2 Physical Model Assembly

When the physical model was in the assembly stage, some details were modified to improve the function of the model. The rotating and horizontal motion of the hose created a binding force on the three-track system. This is likely due to the fact that the supports were not equally spaced every 120° around the hose. An additional support and

counter weight was added, placing the supports every 90° around the hose. Figure 4-9 shows the original physical model set-up. Figure 4-10 shows the circular track that was constructed that allows the hose to rotate as it moves vertically and also the connection to the vertical track. These vertical tracks were lubricated to minimize friction effects.

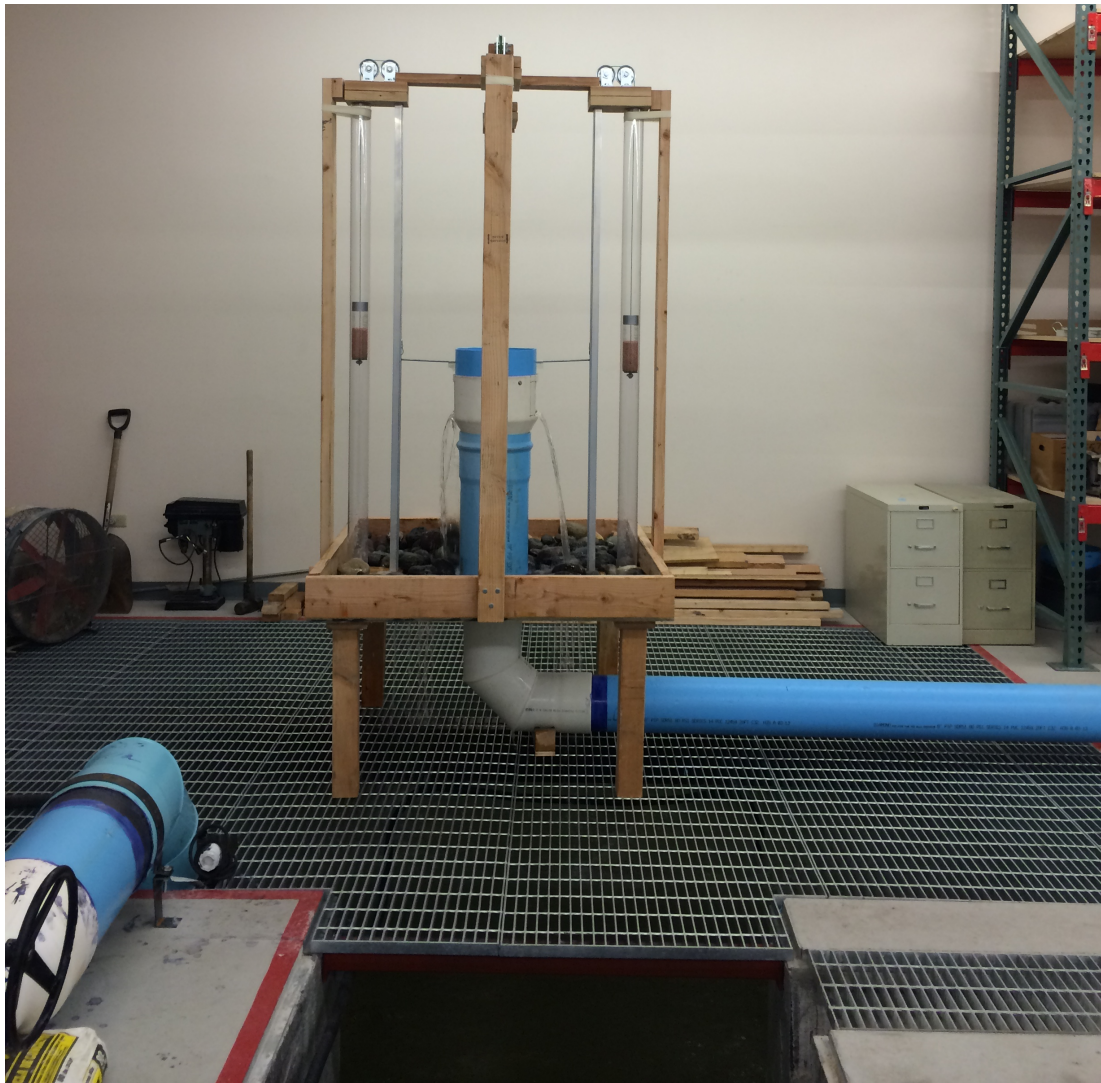


Figure 4-9 Original physical model set-up

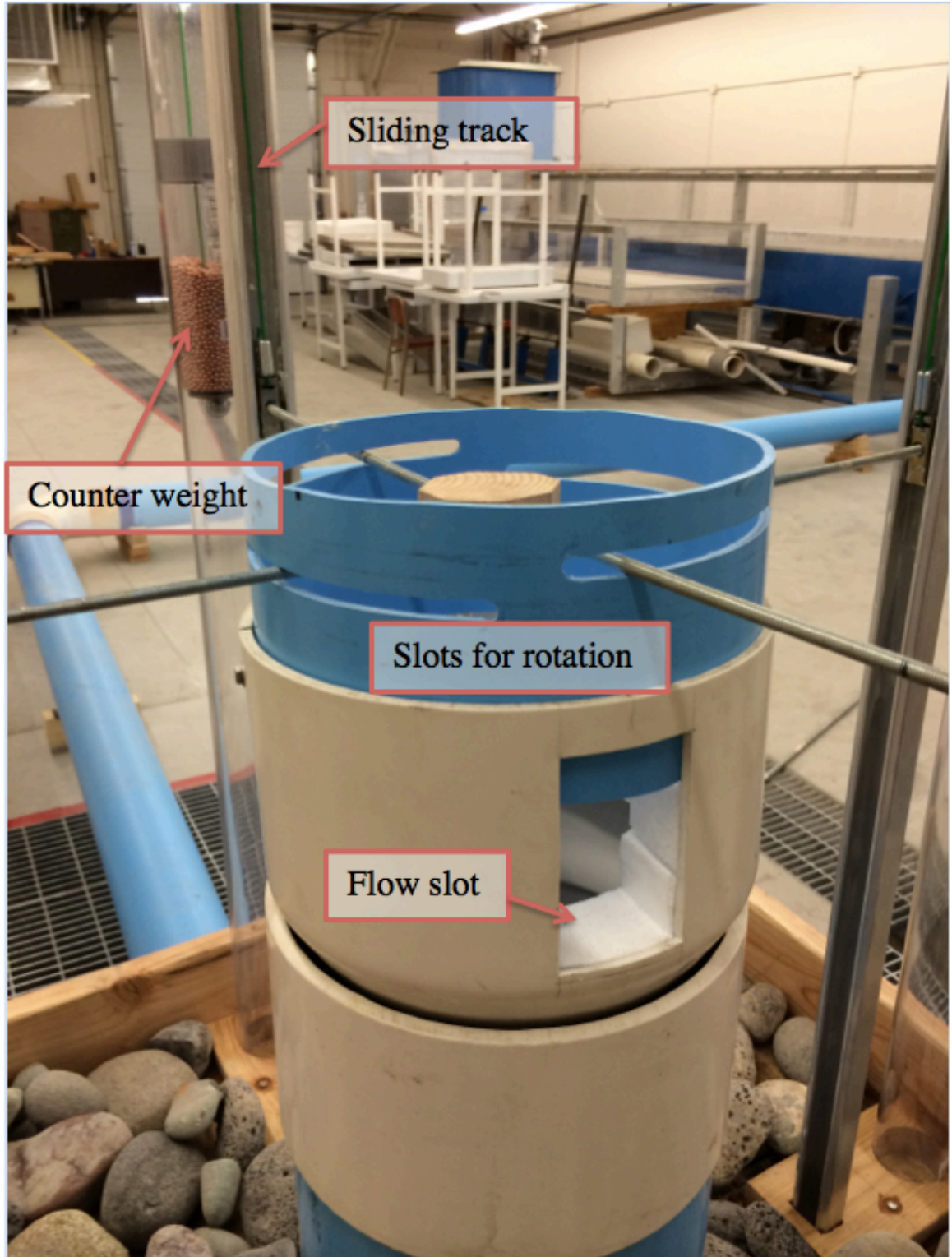


Figure 4-10 The constructed circular track

A 12x8 inch pipe reducer was attached to the top of the flexible hose to provide confinement to the Styrofoam floater. The pipe reducer has two rectangular openings or slots (different sizes have been used for different trials) to allow water to flow out of the regulator. A short section of one-foot pipe was attached at the top of the reducer with slots to create a circular track. To measure the water level inside the pipe and hose a 0.25" clear hose was attached to the main PVC elbow and installed vertically to act as a piezometer.

4.1.2.3 Hose Buckling

The hose was manufactured using a flexible plasticized fabric, which was not able to hold a uniform shape during the expansion due to the water pressure introduced. An enlargement in the hose mid-height appears as the hose starts to expand vertically. The enlargement appears in one side of the hose forcing the floater to lean toward the other side, creating a large amount of friction in the sliding track. Two different hoses with different material strengths were tested but did not solve the problem. One hose was the plasticized fabric and the other was made of thicker clear plastic. Although a stronger hose would have less flexibility, it would also have a smaller expansion ratio; therefore this type of hose was not tested.

To add more restrictions on the rotational movement of the floater, four holes were used instead of the circular track as seen in Figure 4-10. A short 12-inch pipe was placed around the hose for the floater to sit on. Further more, water was added in the space between the hose and the rigid 12 inches pipe to provide confinement for the hose

and counter the water pressure inside the hose (see Figure 4-11). This effort did not prevent the hose from buckling (see Figure 4-12).



Figure 4-11 water outside the hose is used to counter the water pressure inside the hose



Figure 4-12 Hose is buckling with the water counter pressure approach used.

The second method to solve the problem of the bulging hose was to use four 2.5-inch diameter pipes placed around the flow regulator to support the hose as it expanded vertically. The floating Styrofoam was attached inside a short 8-inch pipe section instead of the 12x8 inch reducer. This allowed the four rigid pipes to maintain close contact with the flexible hose in an attempt to minimize bulging of the hose as it expands vertically. This setup is shown in Figure 4-13. Counter weight was not required in this case as the floater provided sufficient buoyancy to lift the pipe when flow was sufficiently high. In addition, the water flow was routed through the flume headbox to minimize flow oscillations that were being created by the pump. Figure 4-14 shows the setup with the water lifting the hose while the hydraulic head increases above the initial starting point of the hose. Even though the rigid pipes provided support for the flexible hose, some buckling still occurred as shown in the figure. It was also noted that friction between the supports and flexible hose limited the motion of the flexible hose. This design used only three components; the hose, the hose floater and the railing to support the hose. The simplicity of this experiment was a key factor, which made it work.

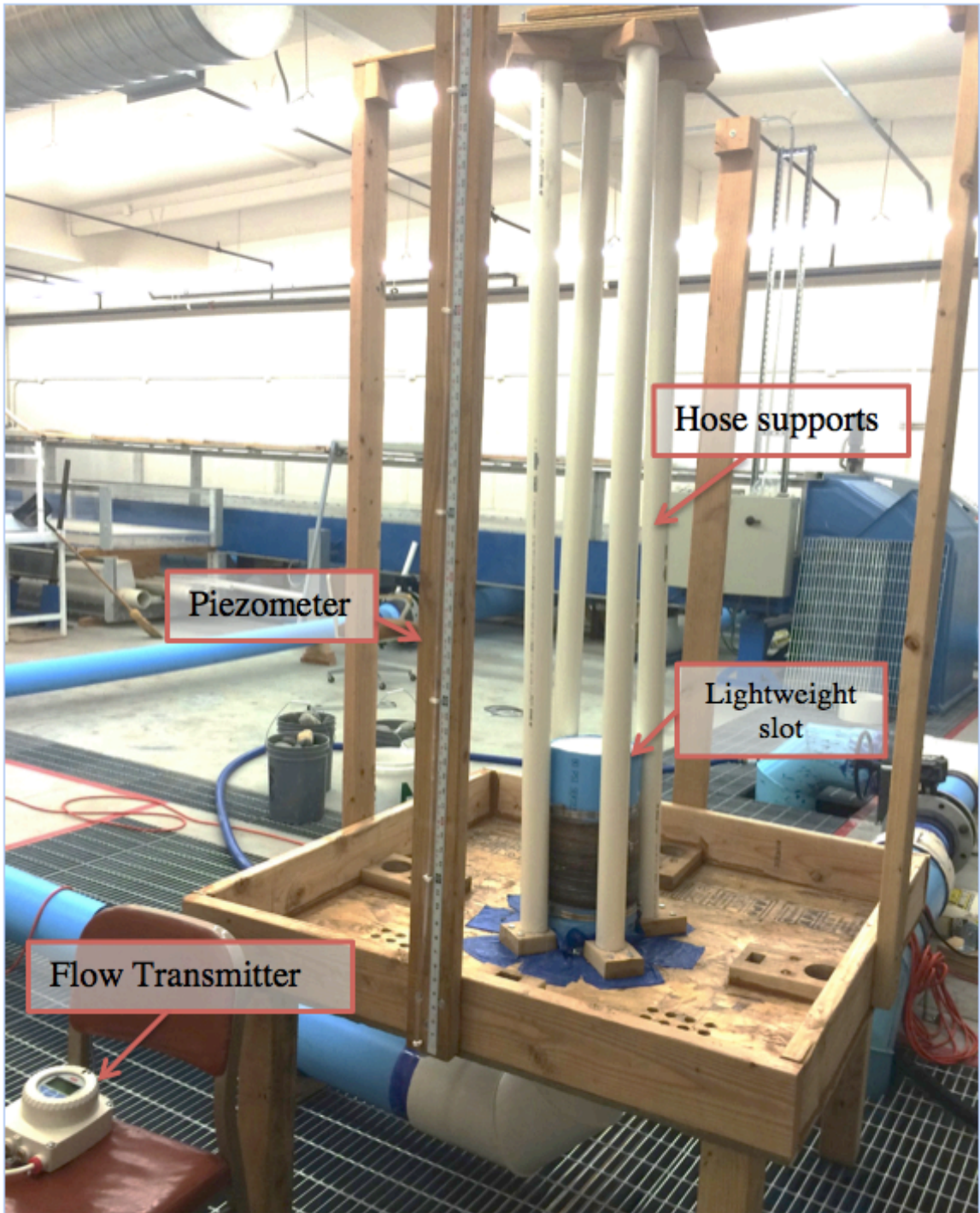


Figure 4-13 Lightweight slot is attached to the floater and the hose is supported by four vertical pipes.



Figure 4-14 Hose is buckling and leaning toward the supporting pipes.

Chapter 5 – Results and Calculations

5.1 Physical Models

The four vertical pipes supporting the hose was the only method that worked when the model was constructed. The simplicity of the model reduced the friction caused by the hose bulging out. Flow measurements were taken using an 8-inch ABB flow meter. The pressure head inside the flexible hose was measured using a 0.25-inch clear tube mounted vertically attached to the setup. The bottom of the water slot is the datum for the head measurements.

When performing the experiment there was a hysteresis effect on the variation in the flow. This effect occurs because the hose leaned sideways against rigid pipes creating friction. When the hose was expanding, friction will act against the hose movement requiring more force to lift the hose. However, when the hose was contracting, the friction force opposed the motion, requiring the pressure head to reduce significantly before it adjusted and lowered. Figure 5-1 shows the result from the physical experiment. Three separate tests were conducted to evaluate the repeatability of the flow regulator. For each trial, the pressure head increment rate was different. As shown in Figure 5-1, there is a considerable scatter and variability in each trial. A ‘best fit’ line was visually placed on the figure, showing the estimated average performance.

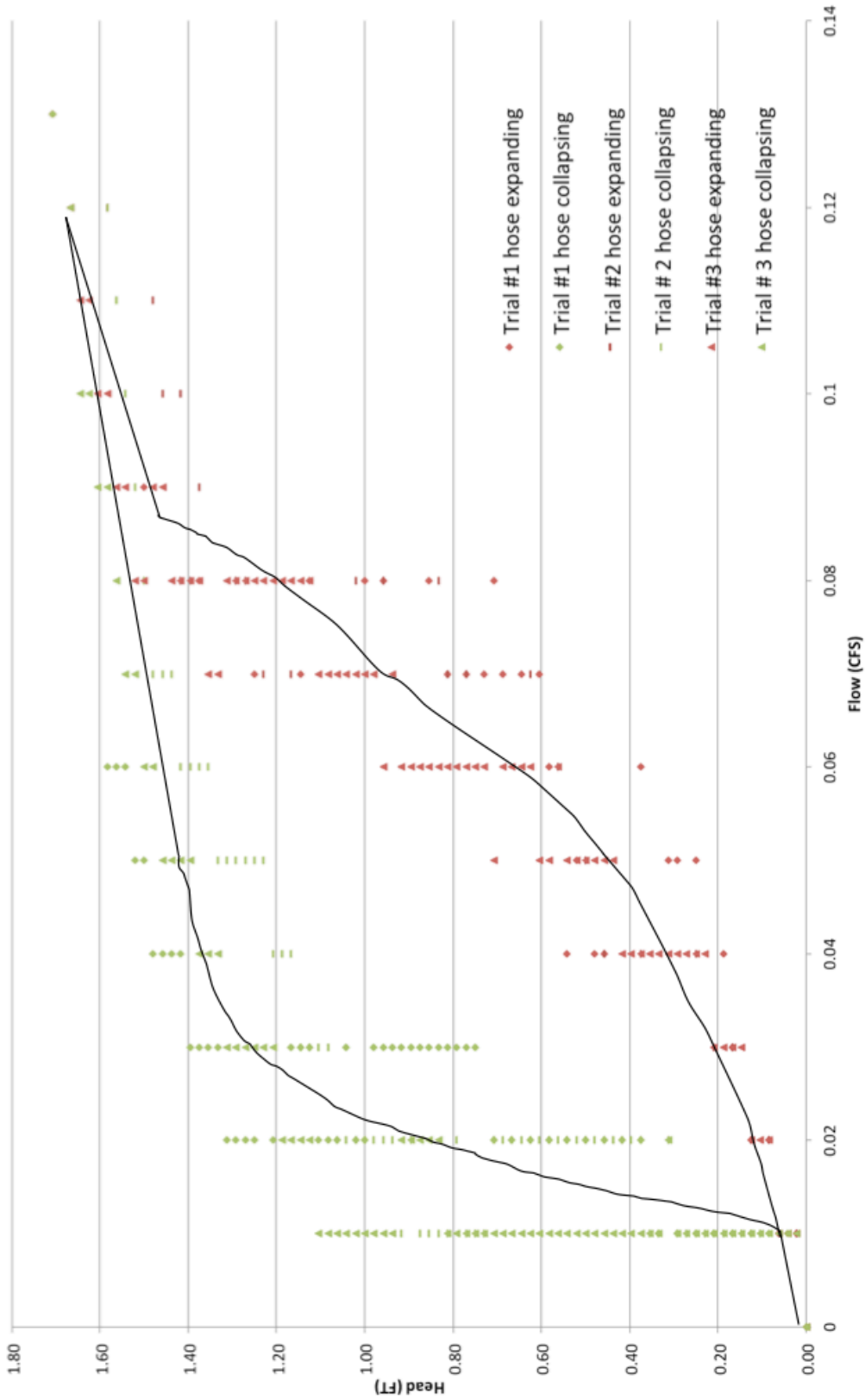


Figure 5-1 The flow regulator, three trials flow output at different pressure head.
 The black line is hand drawing average of the results.

Figure 5-1 shows an increase in the flow until the depth of water above the slot is sufficient to lift the hose at a flow rate equal to 0.02 CFS. The flow stayed semi-constant as the floater adjusted vertically and kept the difference in head pressure between flume headbox head and the slot constant as the float rose. The weight of the hose to be lifted increases because more of the hose is lifted from the table. This requires a slightly greater depth on the float to create more buoyancy force coming from the submerged volume of the floater. Static friction due to the hose buckling and leaning to one side of the rigid pipes made the flow experience a rapid increase, followed by small decrease. The flow kept increasing in a small magnitude until the enlarged section touched one of the rigid pipes creating friction. The flow kept increasing but in a bigger magnitude until it overcame the static friction; the hose jumped, causing a reduction in flow in some cases (see figure 5-1 Trial 3 hose expansion pressure head 0.6 and 0.8 feet). This flow pattern kept going until all the floater depth was consumed or the hose could not expand any more. At that point the device behaved like a simple slot (see figure 5-1 trail 3 hose expansion pressure head 1.4 and 1.7 feet). When draining the tank, the device went though the same flow patterns. The main difference is that the friction force reversed its orientation. This causes an obvious reduction in the discharge rate.

The reason that the flow increases as the pressure head increases is because the buoyancy force is required to lift more of the hose off the base as it expands (See Figure 5-2). The additional weight requires more submerged volume of the floater to counter the force increasing the flow rate. The change in flow can be reduced by using either a lighter hose or a wider floater. A wider floater would reduce the change in flow rate by displacing more volume with a slight change in depth; and thereby increase the buoyancy force.

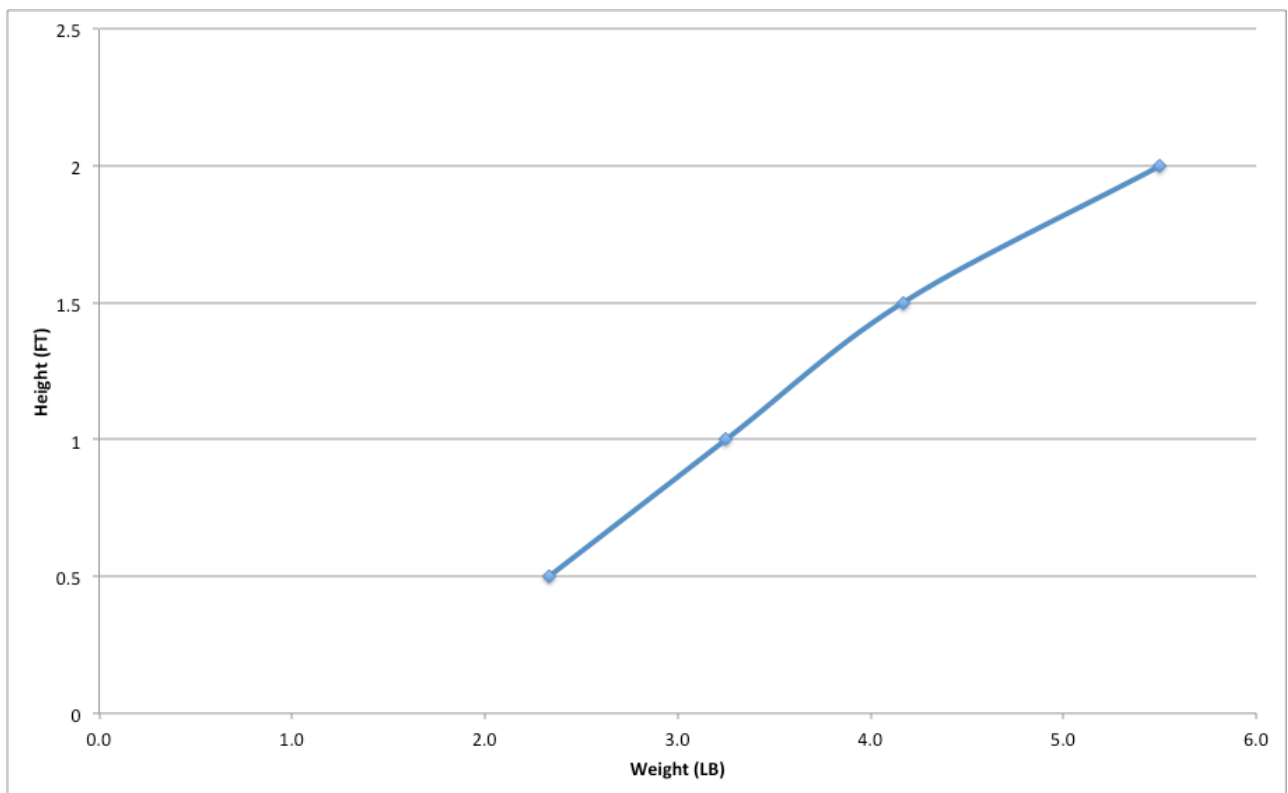


Figure 5-2 The average weight change at different heights

5.2 Weirs Discharge Coefficient

The proposed flow-regulating device is designed so that the water moves vertically to reach the slot that changes the direction of the water streamlines (see Figure 5-3). The stream path has exposed some concerns regarding the reliability of the RSC equation, and whether the weirs discharge coefficient is constant or varying when the hose expands. The RSC equation was developed for a horizontal flow that has flow streams near and below the slot, which are much slower than water above the slot, creating flow losses (see Figure 5-4).

The change in weight of the hose and friction as it moves upward are important factors for varying the flow as the inlet pressure head increases. However, for now the friction and weight change will be ignored, to further understand the effect of the weirs discharge coefficient on the flow rate. Two Flow-3D simulations were set up, and compared against the rectangular sharp crested (RSC) weir's equation. The first simulated a flow over a weir where the flow moves horizontally, which represents the common use of a weir. The simulation of the first setup was copied and calculated again at different heights of the wall under the slot while the water depth above the weir remained the same. The change in the two flows is a factor of the weir discharge coefficient. This data was compared to the data obtained from the series of simulations in Section 4.1.1.2 and the rectangular sharp crested weir's equation. The RSC equation was

used to calculate the flow twice; the pipe height and water depth was synchronized with horizontal flow through the weir simulation. The results of this comparison are displayed in Figure 5-5.

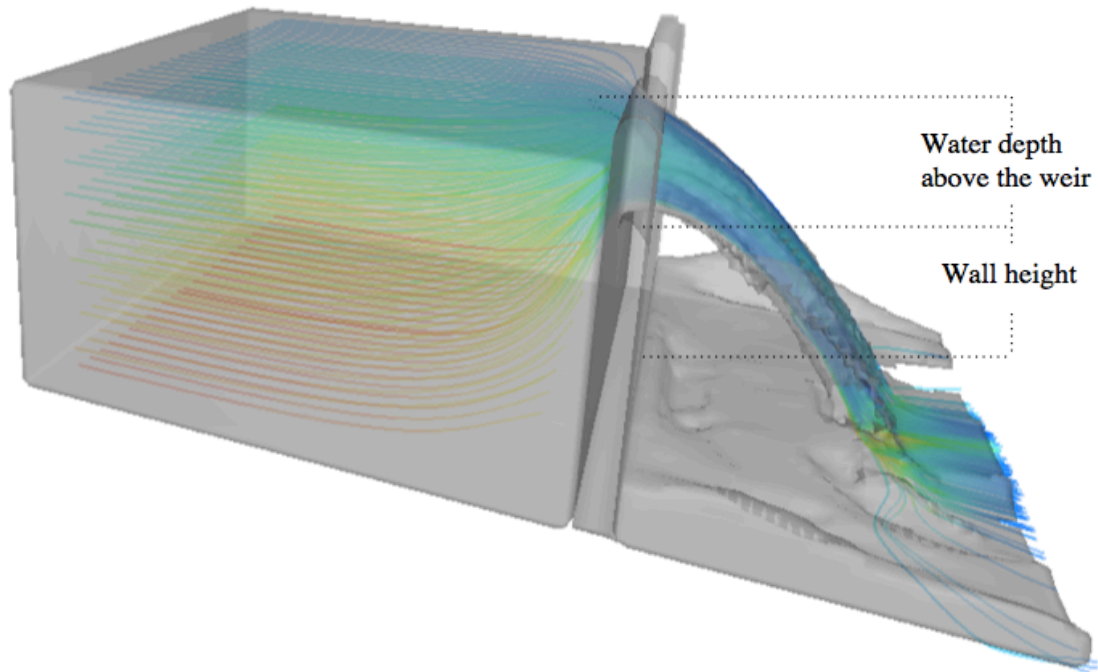
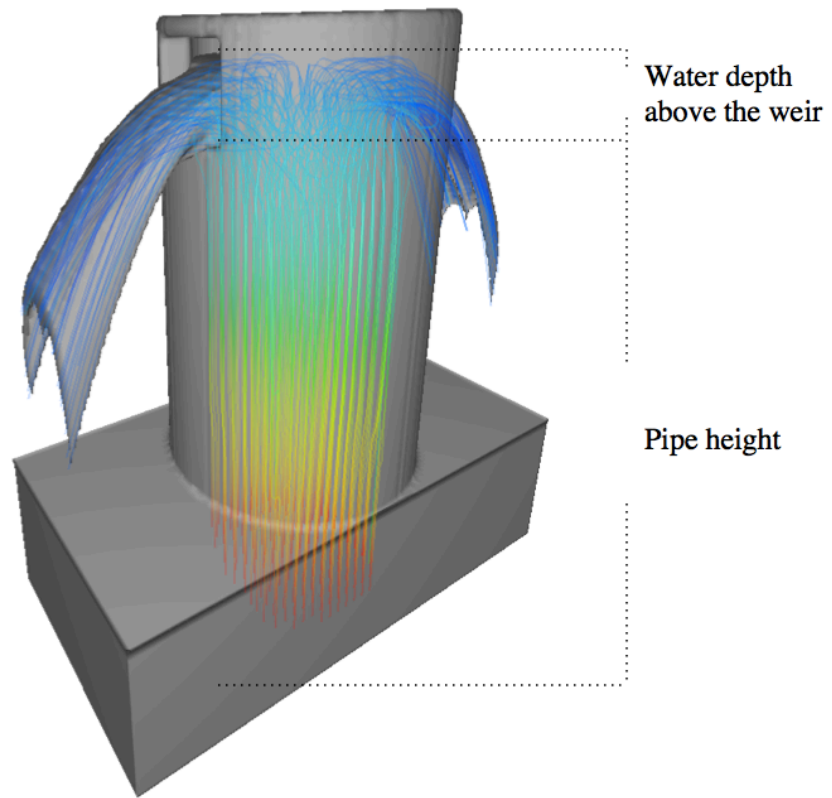


Fig. 5-3 Streamlines showing the flow direction for the horizontal flow.



(B)

Figure 5-4 Streamlines showing the flow direction for the vertical flow (B)

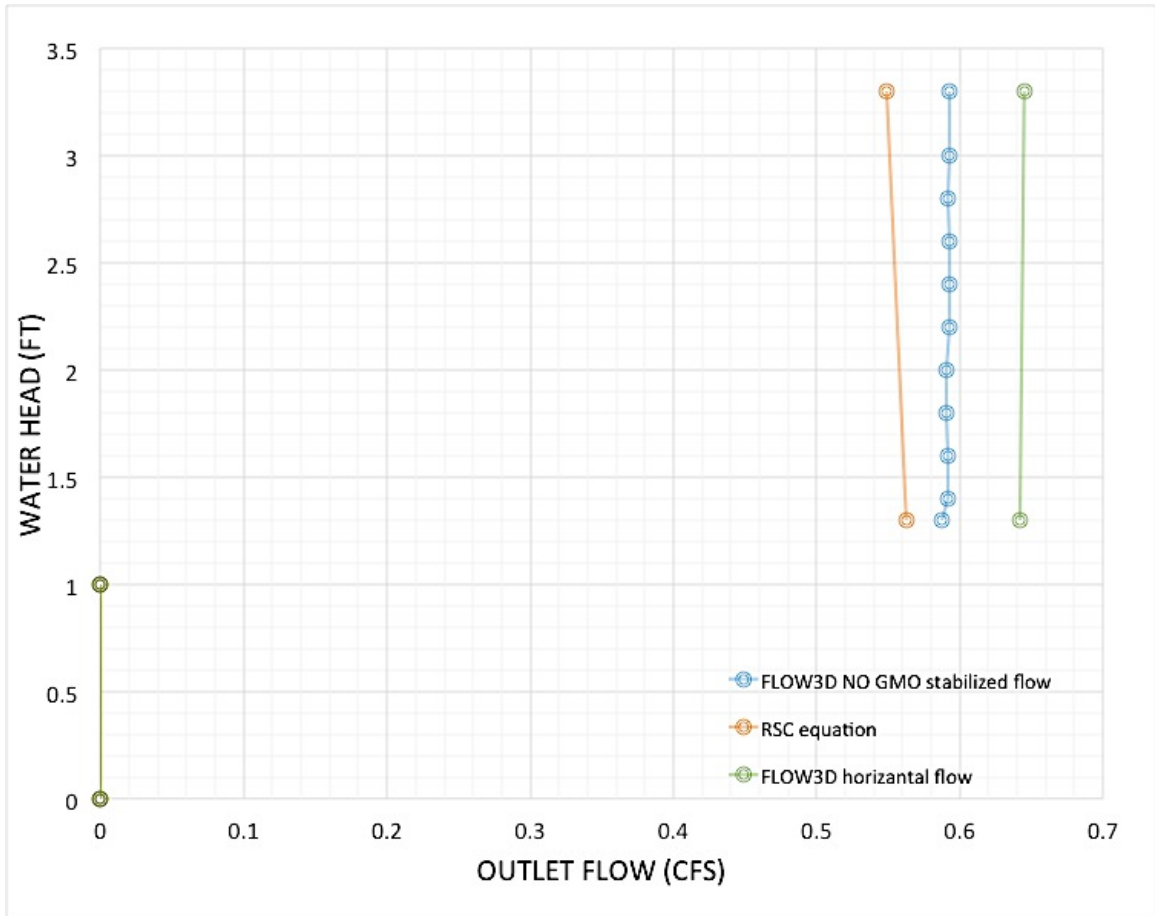


Figure 5-5 Flow rate at different water heads when increasing the pressure head using different methods.

The flow rate increases with increased wall height when Flow-3D is used to calculate the flow for horizontal simulation setup. The results obtained using the RSC equation show a reversed relationship between the wall height and the flow rate. This occurrence needs further physical experimentations to draw a solid conclusion, because the equation's requirements were not met for this slot. For this equation, the slot width

needs to be greater than three times the water height above the slot. The slot designed using Flow-3D was thinner and did not meet this requirement (see Appendix A). On the other hand, the flow rate did not change when a longer pipe was used in the vertical inlet flow, for a Flow-3D series of simulations at different heights. The flow reduction in the horizontal flow simulation occurred due to less shear friction loss, since there is less variation in the water velocity when compared against the short pipe's streamlines.

The constant discharge coefficient (K) used for calculating flow in the RSC equation was 0.64 at its maximum flow. The flow rate came short and did not reach flow predicted when using FLOW-3D. For the proposed water flow regulator, a constant discharge coefficient (K) between 0.64 and 1 is recommended, in order to account for the system losses.

5.3 Comparing the Physical Model Data to RSC Equation Results

All vertical components of the forces on the device influence its outflow. Increased weight due to the floater rising caused the flow to increase. During the physical experiment, the average change in weight was measured to factor the weight change in the RSC equation. Figure 5-6 shows the physical model data compared to RSC equation results when the weight is factored in.

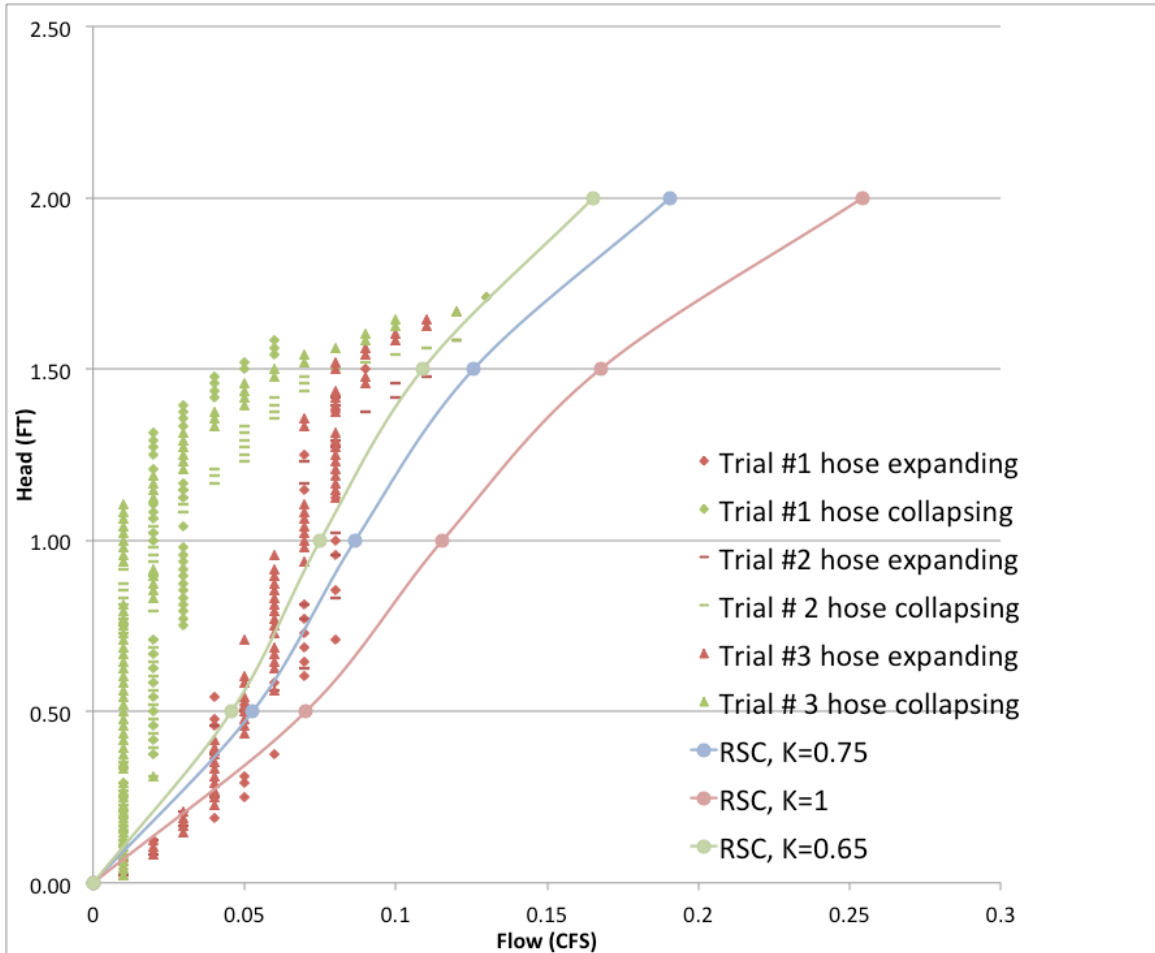


Figure 5-6 Comparing the physical model flow data to the rectangular sharp crest weir equation with weight factored in.

The predicted flow of water using the rectangular sharp crested equation and weirs discharge coefficient equals to 0.65, which is closest to the outflow data obtained from the experiment. Factoring the stagnation pressure into the equation can further enhance the RSC equation results. Water velocity gets converted into upward pressure

when it hits the Styrofoam floater, reducing the flow and the force needed to lift the hose. This force can be calculated using the energy equation. However, since the water velocity is slow the stagnation pressure is ignored. The percentage of flow change was calculated at just below 0.001% (see Appendix C).

Chapter 6 – Conclusions and Recommendations

The simplicity of the design gives it a cost advantage compared to other available flow regulators. The device will require more maintenance; however, it may not require as many labor hours to fully reassemble and repair the device, since it has only three main components (flexible hose, floaters, and a hose railing). The results of the physical model can be further enhanced using a lighter hose, so that as the hose expands, the weight does not vary as much. Also, the buckling can be eliminated by using a reinforced expansion hose specifically designed for increased lateral water pressure as the hose expands vertically.

The hose bracing should also use independent rings implanted in the hose (instead of helix bracing), to prevent the hose from rotating while expanding. To prevent the hose from buckling and leaning toward the railings, every other bracing ring should have four short rods, which would be connected to the tracks. A second option is to use a telescopic pipe instead of the hose. However, counter weight must be used if normal weight PVC pipe is used for the telescopic sliding tubes. The pipes do not have to be tied closely together. However, dripping water must be accounted for in the Discharge Rate vs. Head chart.

The proposed flow regulator is a promising new concept to control the outflow of a detention basin that needs more design refinements and research to optimize its function. For instance, The Styrofoam shape should be optimized to handle trash without increasing the flow variability. The Styrofoam floater should be protected against erosion and weathering using a protection cover. Also, the range of pressure head difference that the device can handle should by expand from almost 2 feet to at least 6 feet of head

difference between the reservoir and its outlet by reducing the frictional force or weight of the device.

References

- Akan, A. (1993). *Urban stormwater hydrology : a guide to engineering calculations*. Lancaster, Pa: Technomic Pub. Co.
- ASCE. (1985). *Stormwater detention outlet control structures: a report of the Task Committee on the Design of Outlet Control Structures of the Committee on Hydraulic Structures of the Hydraulics Division of the American Society of Civil Engineers*. New York, N.Y. (345 E. 47th St., New York 10017-2398: American Society of Civil Engineers. ISBN 0-87262480-3
- Atlanta Regional Council (ARC). *Georgia Stormwater Management Manual Volume 2 Technical Handbook*. 2001.
- British Water. (2005). *Guidance to proprietary sustainable drainage systems and components*. [online] Retrieved from: http://www.ohel.co.uk/wp-content/uploads/2013/07/Tech_Guidance_SUDS.pdf [Accessed: 29 Jan 2014].
- Debo, T. & Reese, A. (2003). *Municipal stormwater management*. Boca Raton, Fla: Lewis Publishers.
- Dermot, O. (2008). *Design and Development of a Radial Vortex Flow Control Device*. Unpublished Master thesis, Dublin City University, Dublin, Ireland, UK.
- Ferguson, B. (1998). *Introduction to stormwater : concept, purpose, design*. New York: Wiley.
- Flammer, G. H., Jeppson, R. W., & Keedy, H. F. (1986). *Fundamental principles and applications of fluid mechanics*. S.I: s.n.
- Flow-3D user manual; excellence in flow modeling software, v 9.4. (2009). FLOW-3D. Flow Sciednce, Inc., Santa FE, NM.
- Georgia stormwater management manual. (2001). Atlanta, Ga.: Atlanta Regional Commission.
- Gribbin, J. (2007). *Introduction to hydraulics and hydrology with applications for stormwater management*. Clifton Park, NY: Thomson Delmar Learning.
- Haestad Methods Engineering Staff. (2004). *Computer applications in hydraulic engineering: connecting theory to practice*. Waterbury, CT: Haestad Press.
- Hardy, P. P. (1968). United States Patent 3,407,839. SELF-REGULATING FLUID FLOW VALVES.
- Hubbart, J. (2008). *History of hydrology*. Retrieved from <http://www.eoearth.org/view/article/1535>

- Hydro International plc, (2012). S-RANGE HYDRO-BRAKE OPTIMUM FLOW CONTROLS." Hydro International. British Board of Agrément.<<http://www.hydro-int.com/>>.[Accessed:05 Feb 2014]
- Hydrok. HydroOslide Flow control Regulators. [Online] Retrieved from: <Http://http://www.hydrok.co.uk/suds/hydroslide.html> [Accessed: 30 Jan 2014].
- J. Burnham. FLOW-3D support engineer. personal communication, April 2, 2014.
- Johnson, M. C., & Savage, B.(2001). Flow over Ogee Spillway: Physical and Numerical Model Case Study. Journal of Hydraulic Engineering.
- Logan, D. (2012). A first course in the finite element method. Stamford, CT: Cengage Learning.
- Martin R. Hendriks (2010), Introduction to Physical Hydrology, Oxford University Press
- McCuen, Richard H. Hydrologic analysis and design. Upper Saddle River, N.J: Pearson Prentice Hall, 2005. Print.
- Olsen, E. (2004). DETENTION BASIN OUTLET STRUCTURE “DBOS”. Unpublished Master thesis, Utah State University, Logan, Utah, USA.
- South Carolina, DHEC (2005). Storm Water Management BMP Handbook <https://www.scdhec.gov/environment/water/swater/docs/wqc-dryPonds.pdf>
- Tu, J., & Yeoh, G. H. (2013). Computational fluid dynamics: a practical approach (Second ed.). Waltham, MA: Butterworth-Heinemann.
- Urbonas, B. & Stahre, P. (1993). Stormwater : best management practices and detention for water quality, drainage, and CSO management. Englewood Cliffs, N.J: PTR Prentice Hall.
- USDA SCS (Soil Conservation Service). 1972. SCS National Engineering Handbook, Hydrology. Washington, DC: USDA. Retrieved form: <ftp://ftp.wcc.nrcs.usda.gov/wntsc/H&H/NEHhydrology/ch15.pdf>

Appendix

A) Flow-3d hand calculations

1) Calculating the density needed to maintain the water depth 0.3 feet above the slat opening

* The weight ring volume

$$V_1 = \pi(0.78^2 - 0.6^2) \times 0.1 = 0.078 \text{ ft}^3$$

* The volume of the cylinder with the slat openings and the floater gap

$$V_2 = \pi(0.78^2 - 0.73^2) \times 0.4 - (0.5 \times 0.4 \times 0.18) + \pi(0.78^2 - 0.73^2) \times 0.1 = 0.3 \text{ ft}^3$$

* The bottom cylinder volume

$$V_3 = \pi(0.78^2 - 0.6^2) \times 0.1 = 0.078 \text{ ft}^3$$

* The submerge volume

$$V_s = \pi(0.73^2 - 0.6^2) \times 0.2 = 0.1086 \text{ ft}^3$$

* Calculating the density of the weight ring using Archimedes law of buoyancy

$$F_B = W$$

$$V_s \times \gamma_w = V_1 \times \gamma_1 + V_2 \times \gamma_2 + V_3 \times \gamma_3$$

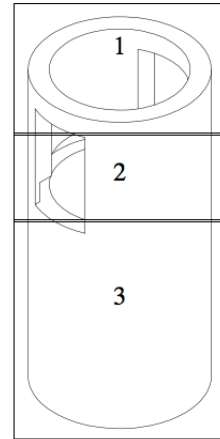
$$\text{Let } \gamma_2 = \gamma_3 = (0.01 \times 32.2)$$

$$0.1086 \times (1.94 \times 32.2) = 0.078 \times \gamma_1 + 0.3 \times (0.01 \times 32.2) + 0.078 \times (0.01 \times 32.2)$$

$$\Rightarrow \gamma_1 = 82.51 \text{ lb/ft}^3$$

$$\rho = \gamma/g$$

$$\Rightarrow \rho_1 = 82.51/32.2 = \boxed{2.56 \text{ slug/ft}^3}$$



2) Hand Calculating the stabilized flow

*The rectangular-sharp-crested weirs equation is used to approximate the outlet flow (Flammer, 1986)

$$Q = K \times \left(\frac{2}{3}\right) \times B \times \sqrt{2g} H^{3/2}$$

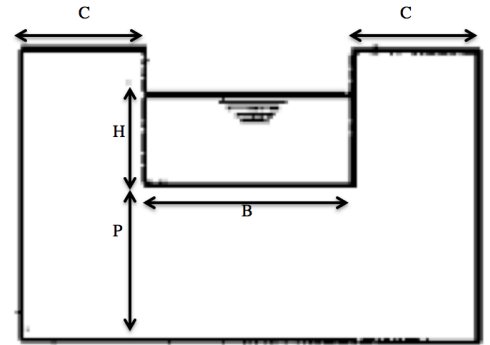
Where,

K = Weirs discharge coefficient

P = the slat height

H = water height above the slot

C = the sides walls length



In order to get a good flow prediction date using the rectangular-sharp-crested weirs equation the slat design should have three requirements:

- 1) P = between 1 feet and 2 feet $> 2H = 0.3 * 2 = 0.6$ **OK**
- 2) $C = (0.73 - 0.5) / 2 = 0.115$ feet $> 2H = 0.6$ **NG**
- 3) $B = 0.5$ feet $> 3H = 0.9$ **NG**

∴ The flow prediction may my not be accurate, however the following calculation will predict how the flow behave as the pipe moves upward reaches the

$$K = 0.605 + 0.08 * \left(\frac{H}{P}\right) + \frac{1}{305 * H}$$

When the flexible pipe just starting to move upward

$$K_{initial} = 0.605 + 0.08 * \left(\frac{0.3}{1}\right) + \frac{1}{305 * 0.3} = 0.640$$

When the flexible pipe reaches the maximum designed height

$$K_{Max\ head} = 0.605 + 0.08 * \left(\frac{0.3}{3}\right) + \frac{1}{305 * 0.3} = 0.624$$

The expected flow at each slat

$$Q_{initial} = 0.640 \times \left(\frac{2}{3}\right) \times 0.5 \times \sqrt{2 \times 32.2} \times 0.3^{3/2} = 0.2813 \frac{ft^3}{s}$$

$$Q_{Max\ head} = 0.628 \times \left(\frac{2}{3}\right) \times 0.5 \times \sqrt{2 \times 32.2} \times 0.3^{3/2} = 0.2743 \frac{ft^3}{s}$$

Because there are two slats in the moving pipe the flow should be multiplied by 2

$$Q_{initial} = 0.2813 \times 2 = 0.5626 \frac{ft^3}{s}$$

$$Q_{Max\ head} = 0.2743 \times 2 = 0.5486 \frac{ft^3}{s}$$

Note that the flow rate is decreasing in a small rate as the flexible pipe rises.

B) Buoyancy force calculations

		Model		
		Flow-3D mode	Model Concept	light weight 8" floater
Floater	Outer diameter(FT)	0.917	0.917	0.6667
	Inner diameter (FT)	0.6667	0.6667	0.0000
	Floater depth (FT)	0.3333	0.3333	0.3333
Slot	Height (FT)	0.3333	0.3333	0.3333
	Width (FT)	0.6000	0.2500	0.1250
Floater volume (FT^3)		0.0036	0.0620	0.0888
Max buoyancy force (LB)		0.2267	3.8707	5.5441
Buoyancy force per liner inch (LB/ IN)		0.0567	0.9677	1.3860

C) Rectangular sharp crested (RSC) weir's equation

Hieght (ft)	0	0.5	1	1.5	2
Hose weight (Lb)	0	2.333333333	3.25	4.16666667	5.5
Max buoyancy force (LB)	5.544104764	5.544104764	5.54410476	5.54410476	5.54410476
Floater depth (in)	4	4	4	4	4
submerge (%)	0	0.420867468	0.58620826	0.75154905	0.99204475
water depth above slot (in)	0	1.683469871	2.34483303	3.0061962	3.96817898
Flow RSC, K=1 (cfs)	0	0.070279366	0.11552812	0.16770492	0.25433533
Flow RSC, K=0.75 (cfs)	0	0.052709525	0.08664609	0.12577869	0.1907515
Flow RSC, K=0.65 (cfs)	0	0.045681588	0.07509328	0.1090082	0.16531796
stagnation pressure (lb/ft^2)	0	8.01151E-07	2.1649E-06	4.5619E-06	1.0492E-05
stagnation Force (lb)	0	2.49221E-06	6.7345E-06	1.4191E-05	3.2639E-05
submerge (%)	0	0.420867018	0.58620704	0.75154649	0.99203886
water depth above slot (in)	0	1.683468073	2.34482818	3.00618596	3.96815543
Flow RSC, K=0.65 (cfs)	0	0.045681515	0.07509304	0.10900764	0.16531649
% of difference in flow stagnation pressure made	0	0.000160214	0.00031082	0.00051089	0.00089017

Sample calculations for the stagnation pressure using RSC equation,
Floater height is 1 ft, K=0.65

$$\frac{P_1}{\gamma} + \frac{V_1^2}{2g} + Z_1 = \frac{P_2}{\gamma} + \frac{V_2^2}{2g} + Z_2$$

$$P_2 = \left(\frac{V_1^2}{2g} \right) \times \gamma$$

$$P_2 = \left(\frac{Q_1^2}{2gA^2} \right) \times \rho \times g$$

$$P_2 = \frac{Q_1^2 \rho}{2 \left[\left(\frac{D}{2} \right)^2 \times \pi \right]^2}$$

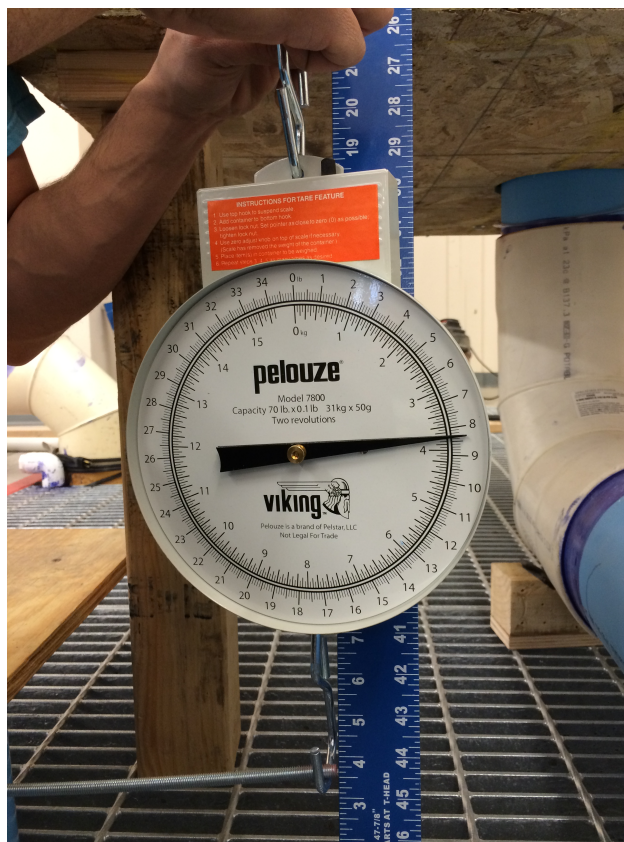
$$P_2 = \frac{0.045^2 \times 1.94}{2 \left[\left(\frac{8}{2} \right)^2 \times \pi \right]^2} = 8.01151E - 07 \frac{lb}{ft^2}$$

B) The physical model

1) List of the model components and their prices:

Item s name	Quantity	Total price
8" Vinyl Hose Duct	1	\$62.78
8" TD9 PVC AIR LIGHT WEIGHT DUCT HOSE	1	\$150
Cable pulley	8	\$38.52*
Pulley Corner/Angle	16	\$59.52
Pulley bolts	8	\$2.52
6' Door slides and track	4	\$292.89 *
8" hose clamp	2	\$22.60
.125" clear hose with fittings	1	\$7.26
3" OD 6' clear pipe	4	\$236.22
8' Tension cable	4	\$9.92
Styrofoam sheets	2	\$10
12"-to-8" pipe reducer	4	\$276.09*
6' Adhesive ruler (water head reading)	1	\$4.82
5/16" bolts and nuts and washers	10	\$8
3/8" bolts and nuts and washers	25	\$20.25
Threaded rods	6	\$15.78
BB capper ammo (weight)	3	\$30
Silicone water seal	1	\$5
Scale	1	\$71.99
8" elbow	2	\$0
20' irrigation pipe, ID 8"	2	\$0
10x6x1.5 inch holders	6	\$0
10x6x1.5 inch cover	3	\$0
Display table	1	\$0
PVC glue	1	\$7.38
Grease	1	\$9.95
Tension cable clamps	4	\$ 8.20
50PK 7in. Small cable ties	1	\$4.99
10PK 48in. heavy duty cable ties	2	\$ 15.94
2PK zinc#10X2-1/2 sheet metal screws	6	\$14.16
6 X 8 ft. Plastic cover	1	\$5.28
Latex sealant	1	\$3.20
50 PK ¼ in. Tubing Mounting Clips	1	\$7.98
Two temperature hot glue gun	1	\$9.98
50 PK 6 in, hot glue sticks	1	\$ 6.57
10 Feet, 2.75" pipes	4	\$29.12

2) Rod deflection



2) Flexible pipe change in weight

